

1 **Seasonal and interannual Dissolved Organic Carbon transport process dynamics in a**
2 **subarctic headwater catchment revealed by high-resolution measurements.**

3 Danny Croghan¹, Pertti Ala-Aho², Jeffrey Welker^{1,3,4}, Kaisa-Riikka Mustonen¹, Kieran
4 Khamis⁵, David M. Hannah⁵, Jussi Vuorenmaa⁶, Bjørn Kløve², and Hannu Marttila²

5 (1) Ecology and Genetics Research Unit, University of Oulu, Oulu, Finland

6 (2) Water, Energy and Environmental Engineering Research Unit, University of Oulu, Oulu,
7 Finland

8 (3) Department of Biological Sciences, University of Alaska Anchorage, USA

9 (4) UArctic, Rovaniemi, Finland

10 (5) School of Geography, Earth and Environmental Sciences, University of Birmingham,
11 Birmingham, UK

12 (6) Finnish Environment Institute, Finland

13
14 Corresponding Author: Danny Croghan (danny.croghan@oulu.fi)

15

16

17

18

19

20

21

22

23

24

25

26

27

28

29

30

31

32

33

34 **Abstract**

35 Dissolved organic carbon (DOC) dynamics are evolving in the rapidly changing Arctic and a
36 comprehensive understanding of the controlling processes is urgently required. For
37 example, the transport processes governing DOC dynamics are prone to climate driven
38 alteration given their strong seasonal nature. Hence, high-resolution and long-term studies
39 are required to assess potential seasonal and inter-annual changes in DOC transport
40 processes. In this study, we monitored DOC at a 30-minute resolution from September 2018
41 to December 2022 in a headwater peatland-influenced stream in Northern Finland (Pallas
42 catchment, 68° N). ~~To~~ Temporal variability in assess-transport processes was assessed using
43 multiple methods, specifically were used: concentration – discharge (C-Q) slope for seasonal
44 analysis, a modified hysteresis index for event analysis, yield analysis, and random forest
45 regression models to determine the hydroclimatic controls on transport. The findings reveal
46 the following distinct patterns: (a) the slope of the C-Q relationship ~~displays~~ displayed a
47 strong seasonal trend, indicating increasing transport limitation each month after snowmelt
48 ~~begins~~ began; (b) the hysteresis index ~~decreases~~ decreased post-snowmelt, signifying the
49 influence of distal sources and DOC mobilization through slower pathways; and (c)
50 interannual variations in these metrics ~~are~~ were generally low, often smaller than month-to-
51 month fluctuations. These results highlight the importance of long-term and detailed
52 monitoring to enable separation of inter and intra annual variability to better understand
53 the complexities of DOC transport. This study contributes to a broader comprehension of
54 DOC transport dynamics in the Arctic ~~because knowledge gained regarding the dominant~~
55 ~~transport mechanisms and their~~, specifically quantifying seasonal ~~variations~~ variability and
56 associated mechanistic drivers, which is ~~is~~ vital for predicting ~~evaluating~~ how the carbon
57 cycle is likely to ~~will~~ change ~~in the future~~ in Arctic ecosystems.

58

59

60

61

62

63

64

65

66 **1. Introduction**

67 The dynamics of Dissolved Organic Carbon (DOC) in Arctic catchments are undergoing
68 profound transformations due to the impacts of climate change, recovery from acidification,
69 and land-use change (Anderson et al., 2023; de Wit et al., 2016; Liu et al., 2022; McGuire et al.,
70 2018; Shogren et al., 2021; Tank et al., 2016). Notably, the Arctic region has experienced a
71 fourfold increase in warming compared to the global average since 1979 (Rantanen et al.,
72 2022), fostering substantial changes in hydrological processes, particularly in terms of
73 transport mechanisms (Liu et al., 2022). Climate change-induced alterations are occurring in
74 permafrost extent (Koch et al., 2022), snowpack water storage (Bokhorst et al., 2016;
75 Pulliainen et al., 2020), snowpack duration (Bowering et al., 2023), snowmelt timing (Tan et
76 al., 2011), and hydrological seasonality (Osuch et al., 2022), which have been significantly
77 affecting DOC dynamics (Liu et al., 2022; Shogren et al., 2021). Consequently, these shifts
78 have triggered rapid and consequential transformations within both the Arctic water and
79 carbon cycles that are both climatically sensitive (Bintanja and Andry, 2017; Bruhwiler et al.,
80 2021; McGuire et al., 2009; Vihma et al., 2016).

81 DOC transport processes (referring to the mobilization of DOC from catchment sources to
82 the stream through differing flow paths) in the Arctic exhibit pronounced seasonality and
83 are highly susceptible to change (Bowering et al., 2023; Csank et al., 2019; Shatilla and
84 Carey, 2019). Among the various transport mechanisms, the spring snowmelt flood is the
85 main event and control on annual DOC flux in Arctic catchments (Croghan et al., 2023).
86 Several studies have demonstrated its contribution ranging from 37% to 82% of the annual
87 DOC load, albeit with considerable variations between catchments and years (Dyson et al.,
88 2011; Finlay et al., 2006; Prokushkin et al., 2011). However, in the Arctic, climate change is
89 reducing snow cover duration and increasing the fraction of precipitation in the liquid phase
90 (Bintanja and Andry, 2017). Consequently, storm events are emerging as increasingly
91 important mechanisms for the export of DOC from terrestrial ecosystems (i.e. soils
92 catchments to streams-stream networks (Day and Hodges, 2018; Speetjens et al., 2022).
93 Furthermore, the lengthening growing seasons, accompanied by potential increases in DOC
94 source supply, are further exacerbating the impact of summer and autumn storm events on
95 DOC dynamics in the Arctic region (Bowering et al., 2020; Pearson et al., 2013). Additionally,

96 while the significance of shoulder seasons (defined in the Arctic as the transitional period
97 between the end of plant senescence and the freezing of the headwaters, and after the
98 onset of thaw till the end of snowmelt) for DOC export has been acknowledged in recent
99 years, their characterization remains limited. Therefore, there is a pressing need for more
100 extensive documentation to elucidate the influence of shifting climate on DOC dynamics in
101 the Arctic (Shogren et al., 2020).

102 Headwater catchments play a crucial role in the transport of DOC into streams (Fork et al.,
103 2020; Lambert et al., 2014). These catchments constitute approximately 90% of the total
104 global stream length and serve as the primary connection for carbon transport between
105 terrestrial landscapes and oceans (Argerich et al., 2016; Li et al., 2021). Allochthonous inputs
106 into the stream, driven by rain and snowmelt events, dominate the dynamics of headwater
107 catchments (Billett et al., 2006; Laudon et al., 2004). Headwater wetland mires are
108 especially abundant in northern latitudes and are significant contributors of carbon to the
109 stream, often exhibiting higher concentrations compared to other landscape types
110 (Campeau and del Giorgio, 2014; Dick et al., 2015; Gómez-Gener et al., 2021). Furthermore,
111 the seasonal dynamics of carbon transfer processes in headwater wetlands differ
112 significantly depending on the season. During snowmelt, rapid superficial pathways are
113 observed, which later evolve into more complex pathways in the landscape during the
114 summer and autumn (Croghan et al., 2023; Laudon et al., 2011). Additionally, headwater
115 catchments are highly vulnerable to the impacts of hydrological extremes (Koch et al.,
116 2022), and they are expected to undergo significant changes due to climate change (Ward et
117 al., 2020). The increasing hydrological stochasticity in Arctic catchments (e.g. occurrence
118 and magnitude of extremes) highlight the need to better understand inter-annual variability
119 using more highly resolved data to characterize event dynamics (Bring et al., 2016).

120 Consequently, longer term and higher frequency study of sensitive headwater catchments is
121 essential to better understand their functioning and response to environmental changes,
122 especially in high latitude conditions (Bruhwiler et al., 2021; Marttila et al., 2022, 2021).

123 To comprehensively investigate the transport processes of DOC across seasons, it is
124 essential to employ high-resolution, long-term monitoring approaches (Shogren et al.,
125 2020). This need is particularly pronounced in headwater environments, where the majority
126 of the DOC input into streams occurs during storm events and snowmelt (Billett et al.,

2006). Only through high-frequency monitoring can we adequately identify and understand the transport processes and characteristics associated with sudden episodic and unpredictable storm and snowmelt events, capturing the necessary resolutions for improved process understanding (Blaen et al., 2016). Furthermore, higher-resolution data collection can facilitate the use of multiple analytical techniques, such as hysteresis analysis, which can offer deeper insights into DOC transport dynamics (Croghan et al., 2023; Lloyd et al., 2016b). Historically, limited spatial and temporal field sampling has led to biases in our understanding of the impacts of climate change in Arctic regions (Metcalfe et al., 2018; Shogren et al., 2020). Additionally, high-frequency DOC measurements in the Arctic remain relatively rare, especially datasets that cover the shoulder seasons and encompass multi-year measurements for assessing inter-annual differences (Beel et al., 2021; Shogren et al., 2021). ~~Hence, there is an urgent need to integrate high-frequency monitoring sites in subarctic, low Arctic, and high Arctic regions, particularly for evaluating the ongoing evolution of the Arctic carbon and water cycles (Laudon et al., 2017; Marttila et al., 2021; Pedron et al., 2023).~~

The rapid evolution of controlling DOC processes due to climate change necessitates and emphasizes pressing the need to document transport processes in understudied high-latitude headwater catchments (Shatilla et al., 2023). The scarcity of multi-year, high-frequency datasets in these high-latitude catchments has impeded our understanding of seasonal and inter-annual DOC dynamics. As the underlying drivers of DOC transport processes are undergoing substantial changes, there is a need to understand baseline levels of variability (Shatilla and Carey, 2019; Shogren et al., 2021). This is particularly essential for assessing the dynamic evolution of the Arctic carbon and water cycles, underscoring the need for a concerted effort to address these knowledge gaps. (Laudon et al., 2017; Marttila et al., 2021; Pedron et al., 2023). To address key knowledge gaps in Arctic headwater DOC transport, our study focused on a peatland-influenced headwater catchment located in subarctic, Northern Finland (68°N), with the overarching aim to identify the ~~primary~~ drivers of DOC transport processes ~~of DOC~~ and explore their seasonal and interannual dynamics. We utilized a unique four-year high-resolution dataset of DOC, allowing us to ~~conduct high-frequency~~ undertake varied analyses. To enhance understanding of DOC transport processes

157 in the Arctic and their implications for future dynamics the following interlinked research
158 questions were addressed:

159 1) How do the main drivers of DOC transport processes vary across different seasons?

160 2) To what extent do DOC transport processes and their drivers vary inter-annually?

161 We hypothesized that:

162 H₁ At the intra annual scale, DOC transport processes would significantly differ between
163 snow melt, snow free, and snow cover seasons;

164 H₂ At the inter annual scale, the metrics of DOC transport processes would significantly
165 differ between years with the most different hydrometeorological conditions.

166

167 **2.0 Methods**

168

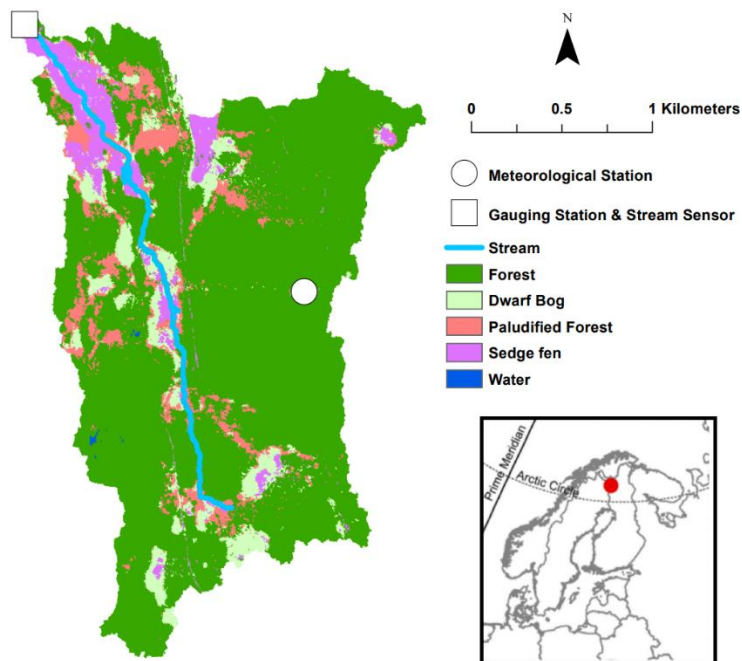
169 **2.1 Site Description**

170 The research was conducted within the Lompolojängänoja catchment, also referred to as
171 the Pallas catchment (Marttila et al., 2021), situated in a peatland-influenced headwater
172 stream (Figure 1). This catchment is located in Northern Finland (68°02'N, 24°16'W) within
173 the Pallas-Yllästunturi National Park. Encompassing a total area of 4.42 km², the Pallas
174 catchment exhibits elevations ranging from 268 m to 375 m above sea level.

175 The stream location is strongly influenced by a peatland, which comprises fens, mires,
176 paludified forest and floodplains. This peatland exerts significant control over the flow
177 dynamics within the catchment, contributing most of the flow at the headwater location
178 (Marttila et al., 2021). Within the broader catchment area, coniferous forests account for
179 79% of the land classification, followed by mixed forests (9%) and peatbogs (8%).

180 The Pallas catchment is categorized as subarctic, characterized by long winters with
181 substantial snowfall and short, rainy summers. Notably, despite its northern latitude, the
182 catchment lacks a permafrost layer, making it one of the most northern research
183 catchments without permafrost (Marttila et al., 2021). The mean annual rainfall in the
184 catchment amounts to 521 mm, with 42% of that precipitation occurring as snowfall.
185 Typically, snowmelt occurs towards the end of April or early May and concludes by late May
186 or early June. Permanent snow cover in the catchment typically commences around late

187 October, though it can extend into late November. For further comprehensive descriptions
188 of the Pallas catchment's characteristics, please refer to Marttila et al., (2021).



189
190 **Figure 1** – Map of the study location (inset), catchment and measurement locations within
191 the catchment. Classification of vegetation in the catchment was derived from (Räsänen et
192 al., 2021)

193 **2.2 Stream Monitoring**

194 The monitoring of stream variables was conducted during the period from 18th September
195 2018 to 31st December 2022. To measure these variables, a multiparameter sonde (YSI-
196 EXO3; Excitation 365 nm, Emission 480 nm) was deployed at the catchment outlet in the
197 Lompolojängänoja stream (Figure 1). The sonde collected data at 30-minute intervals,
198 measuring fluorescent dissolved organic matter (FDOM), electrical conductivity, turbidity,
199 water temperature, and pH. The Finnish Environment Institute (SYKE) installed, calibrated,
200 and maintained the sensor throughout the study duration. Stream flow was measured at
201 the same location using a pressure transducer at a 120° V-notch weir, and records were
202 logged at the same temporal resolution.

203 The FDOM measurements from the sonde were used to model the concentration of DOC.
204 The instrument internally corrected for temperature effects (i.e. thermal quenching), and
205 FDOM ~~required was further~~ corrected for turbidity effects (Downing et al., 2012).

206 Corrections for turbidity were undertaken using the following equation which was derived
207 using internal lab calibration of the instrument:

$$208 \quad DOC_{corrected} = \left(\frac{0.117 \cdot fDOM}{1 - (1.1 \cdot Turbidity) / (120 + Turbidity)} \right) \quad (1)$$

209 Here, the value 0.117 represents the slope obtained from the lab sample DOC against
210 instrument FDOM. To ensure data accuracy, regular grab samples were taken throughout
211 the study (Supplementary Figure 1). No correction was applied to the instrument for inner-
212 filter effects, as there was no observed deviation from linearity in the relationship between
213 in-stream Absorbance 254nm and stream DOC. The instrument underwent regular manual
214 cleaning every two weeks to prevent fouling, while the sensor also had a self-brushing anti-
215 fouling system. No fouling was apparent over the course of the study.

216 The calculation of DOC load during the study period was performed using the following
217 equation:

$$218 \quad C_l = C_c \cdot Q \quad (2)$$

219 Where C_l is the carbon load (mg h^{-1}), C_c is the carbon concentration (mg L^{-1}), and Q is the
220 stream flow (L h^{-1}).

221 Throughout the study, various meteorological measurements were collected. A
222 meteorological station located at the Kenttäröva forest site (Figure 1) was utilized to record
223 precipitation, snow depth, and air temperature in 10 minutes resolution. The maintenance
224 of the meteorological station was carried out by the Finnish Meteorological Institute (FMI).

225 **2.3 Data Analysis**

226
227 The 4-year dataset was transformed into hourly data by calculating hourly means. In our
228 analysis, we delineated three distinct seasonal periods: the snowmelt season, snow-free
229 season, and snow cover season.

230 The snowmelt season was defined as the period starting from the onset of snowmelt,
231 indicated by a decline in snow depth ~~concurrent~~ with a concurrent ~~an~~ increase in flow, until
232 ~~there was no remaining~~ snow cover at the Kenttäröva site reached 0 cm (Fig. 1). The spring

233 snowmelt season was classified using both snow depth and flow as snow depth alone varies
234 for reasons not due to melting (e.g. snowpack consolidation). -The snow cover season
235 referred to the period when permanent snow cover occurred (i.e. the point of the year
236 snow depth was > 0 cm till the spring snowmelt)~~snow cover was present and persisted until~~
237 ~~the subsequent, snowmelt season~~. The snow free season referred to the period between
238 the snowmelt and snow cover seasons where snow depth was 0 cm. All analyses were
239 performed using R in RStudio (version 2023.03.0).

240 To conduct event-based analysis, we extracted specific events from the dataset. Events
241 were defined as periods where discharge had to exceed baseflow by 10% for a duration of
242 at least 24 hours, following definitions used in previous studies (Shogren et al., 2021;
243 Vaughan et al., 2017). Baseflow was computed using a Lyne-Hollick baseflow filter
244 implemented in the R package "grwat". In total, 92 events were identified and extracted
245 from the dataset. Among these events, 18 occurred during the snowmelt period, 63 took
246 place during the snow-free period, and 11 events were observed within the snow cover
247 period.

248 Concentration-Discharge (C-Q) analysis was performed to examine variations in transfer
249 processes at seasonal scales. We calculated the slope (β) of the logarithmic relationship
250 between DOC and streamflow (Q) for each year and each ~~month~~season of the study. The
251 months of December to March were not included in the seasonal analysis as flow remained
252 at baseflow during these months throughout the study. A positive slope ($\beta > 0$) suggests a
253 transport-limited relationship, indicating that the concentration of DOC is primarily
254 controlled by the transport processes. Conversely, a negative slope ($\beta < 0$) suggests a
255 source-limited relationship, indicating that the concentration of DOC is primarily influenced
256 by the sources within the catchment. A slope of zero ($\beta = 0$) indicates chemostasis,
257 indicating no significant change in DOC concentration with variations in streamflow. C-Q
258 slopes have been widely employed to assess the extent of transport or source limitation in
259 catchments (Godsey et al., 2009; Zarnetske et al., 2018). The coefficient of variation (CV) for
260 monthly DOC was also calculated alongside monthly C-Q slopes to identify the amount of
261 variation in DOC relative to changes in C-Q slope.".

262 Hysteresis analysis was conducted to gain insights into flow pathways and transport
263 processes at event scale. The Modified Hysteresis Index (HI) was calculated following Lloyd

264 et al., (2016b). Briefly, the HI is calculated by subtracting the falling limb standardised DOC
265 value from the rising limb standardised DOC value at each 20th flow percentile across the
266 loop. The HI is then calculated as the average HI of the loop for each event. ~~Only single-~~
267 ~~peak events, where the flow returned to at or near baseflow, were selected for analysis~~For
268 each event, individual peaks were treated as separate events to allow the HI to be
269 calculated across the rising and falling limb of the flow. Therefore, for multi-peak events,
270 multiple HI were calculated. The HI yielded values between -1 and 1 for each event. Positive
271 values (> 0) indicate clockwise hysteresis, where the peak concentration of DOC occurs on
272 the rising limb of the event. This pattern suggests the presence of near-stream sources or
273 rapid transport of DOC. Negative values (< 0) indicate anticlockwise hysteresis, where the
274 peak concentration of DOC occurs on the falling limb of the event. This pattern indicates the
275 influence of distal sources or slow transport of DOC (Lloyd et al., 2016b; Williams, 1989).

276 DOC load yields and event water yields were calculated for each event by totalling the sum
277 of DOC (measured in kg per km²) and water (measured in mm), and subsequent linear
278 regressions were performed to assess the variability between DOC and event water yields
279 across seasons and years (Vaughan et al., 2017). For comparisons between years, 2018 was
280 excluded as data collection only began in September 2018. Differences in the linear
281 regression relationships signify variations in transport limitation and source activation
282 dynamics among seasons and years. Furthermore, the Yield Ratio, defined as the ratio of
283 event DOC load yield to event water yield, was computed to identify potential variations
284 between months, indicating differences in transport processes (Vaughan et al., 2017).

285 To identify the best performing hydrometeorological predictors-drivers of event-based
286 metrics, we employed a machine learning method (Random Forest regression) using the R
287 package “*randomForest*”. This approach was chosen due to observed non-linearity in some
288 of the relationships. We considered a set of hydrometeorological predictors based on their
289 potential significance in prior studies examining stream nutrient concentrations-transport
290 processes across seasonal timescales (Blaen et al., 2017). The selected predictor variables
291 included maximum discharge, 7-day antecedent rainfall, average air temperature during the
292 event, average water temperature during the event, and total rainfall during the event.

293 The Random Forest regressions were conducted using the entire dataset, as the aim was to
294 identify the most informative predictors. Models (names in brackets) were created to assess

295 the best predictors of Maximum event DOC (MaxDOC), the percentage of change of DOC
296 during events (DOC Change), event C-Q slope (Slope), event hysteresis index (HI), and event
297 Yield Ratio (Yield Ratio). We present the output of the models for the best predictors, as
298 determined by node purity. Higher node purity values indicate better prediction
299 performance. Additionally, we report the variance explained and the mean of squared
300 residuals for each model. These metrics provide insights into the predictive power and
301 goodness of fit of the selected predictors. Only models with variance explained > 10% are
302 featured. Resultantly, no HI models are featured, as they did not meet this threshold.

303 **3.0 Results**

304

305 **3.1 Time Series**

306 Flow exhibited a pronounced seasonal pattern (Fig. 2a). Each year, the highest flow occurred
307 during the snowmelt season. In the snow-free season, flow was primarily driven by episodic
308 precipitation events. During the early snow cover season, flow was responsive to some
309 precipitation events, but remained at baseflow for most of the snow cover season (Table 1).

310 DOC concentrations (Fig. 2b; Table 1) generally exhibited a consistent rise throughout the
311 snowmelt season, and remained elevated throughout the snow-free period, albeit with
312 frequent event-driven peaks. During the snow cover period, DOC levels initially declined and
313 then stabilized. DOC load, on the other hand, mirrored the dynamics of flow, and the
314 highest loads occurred during the snowmelt season, with smaller event-driven peaks during
315 the snow-free season.

316 Air temperature (Fig. 2c; Table 1) during the snowmelt season exhibited a positive trend,
317 with some variation around 0 °C meaning regular fluctuation between melting and freezing
318 in the snowmelt season. In the snow-free season, temperatures increased until August and
319 then declined. At the onset of the snow cover season, temperatures dropped below zero.

320 Snow cover typically began in mid-October and reached its peak in March or early April.

321 Water temperature (Fig. 2d; Table 1) remained relatively stable during most of the
322 snowmelt season and gradually increased towards the end of the period. Throughout the
323 snow-free season, water temperature closely tracked air temperature. During the snow
324 cover season, water temperature hovered around 0 °C. Turbidity, on the other hand, peaked

325 during the snowmelt season due to initial flushes, but also reached high levels during large
 326 summer events in the snow-free season.

327 When considering the total annual cumulative DOC load averaged across the study (Fig. 2e;
 328 Table 1), the ~6 week snowmelt period contributed around 33.4% of the total annual DOC
 329 load. In contrast, the snow-free season contributed approximately 59% of the total annual
 330 DOC load, while the snow cover season contributed around 7.6%.

331 **Table 1** – Hydrometeorological variables in the snow cover, snow melt, and snow free
 332 seasons. Values are presented as Mean, except for precipitation, which is shown as the total
 333 for each season. ± Standard Deviation.

Year	Season	Turbidity (NTU)	DOC (mg L ⁻¹)	DOC Load (kg h ⁻¹)	Flow (L s ⁻¹ km ⁻²)	Precipitation (mm)	Snow Depth (m)	Water Temp (°C)	Air Temp (°C)
2018	SnowCover	0.86	4.11	0.32	3.90	98.7	0.17	0.25	-4.78
2018	SnowFree	0.90	6.82	0.94	7.16	58	0.02	2.33	1.47
2019	SnowCover	1.31	3.90	0.23	3.10	295.5	0.59	0.19	-7.80
2019	SnowFree	0.68	7.92	2.06	12.81	335.6	0.00	8.39	9.07
2019	SnowMelt	1.60	6.57	3.41	26.76	37.8	0.42	1.70	4.30
2020	SnowCover	0.75	4.30	0.46	4.77	348.4	0.74	0.17	-4.94
2020	SnowFree	0.62	6.88	2.06	13.61	310.6	0.00	10.41	10.51
2020	SnowMelt	1.11	7.20	7.27	47.20	17.5	0.81	1.94	5.14
2021	SnowCover	0.46	4.58	0.73	6.76	304.2	0.63	0.17	-8.21
2021	SnowFree	0.83	6.31	1.21	9.19	289.2	0.00	9.81	10.55
2021	SnowMelt	1.43	6.21	3.92	30.55	74.1	0.67	1.65	2.31
2022	SnowCover	0.98	3.48	0.37	5.63	229.1	0.65	0.17	-6.90
2022	SnowFree	0.89	6.45	1.70	13.50	350.4	0.00	10.26	10.00
2022	SnowMelt	1.31	5.76	4.36	35.11	42.3	0.76	1.79	3.44
Measurement		Snow-Cover			Snow-Melt		Snow-Free		
Flow (L s ⁻¹ km ⁻²)		4.89 ± 4.06			34.38 ± 35.77		12.05 ± 10.90		
DOC Concentration (mg L ⁻¹)		4.03 ± 0.99			6.39 ± 1.12		6.84 ± 1.47		
DOC Load (kg h ⁻¹)		0.41 ± 0.50			4.62 ± 5.26		1.71 ± 1.98		
Air Temperature (°C)		-6.74 ± 6.03			3.62 ± 5.37		9.51 ± 6.08		
Water Temperature (°C)		0.18 ± 0.14			1.76 ± 3.14		9.31 ± 4.31		
Turbidity (NTU)		0.91 ± 0.62			1.37 ± 0.88		0.77 ± 0.52		

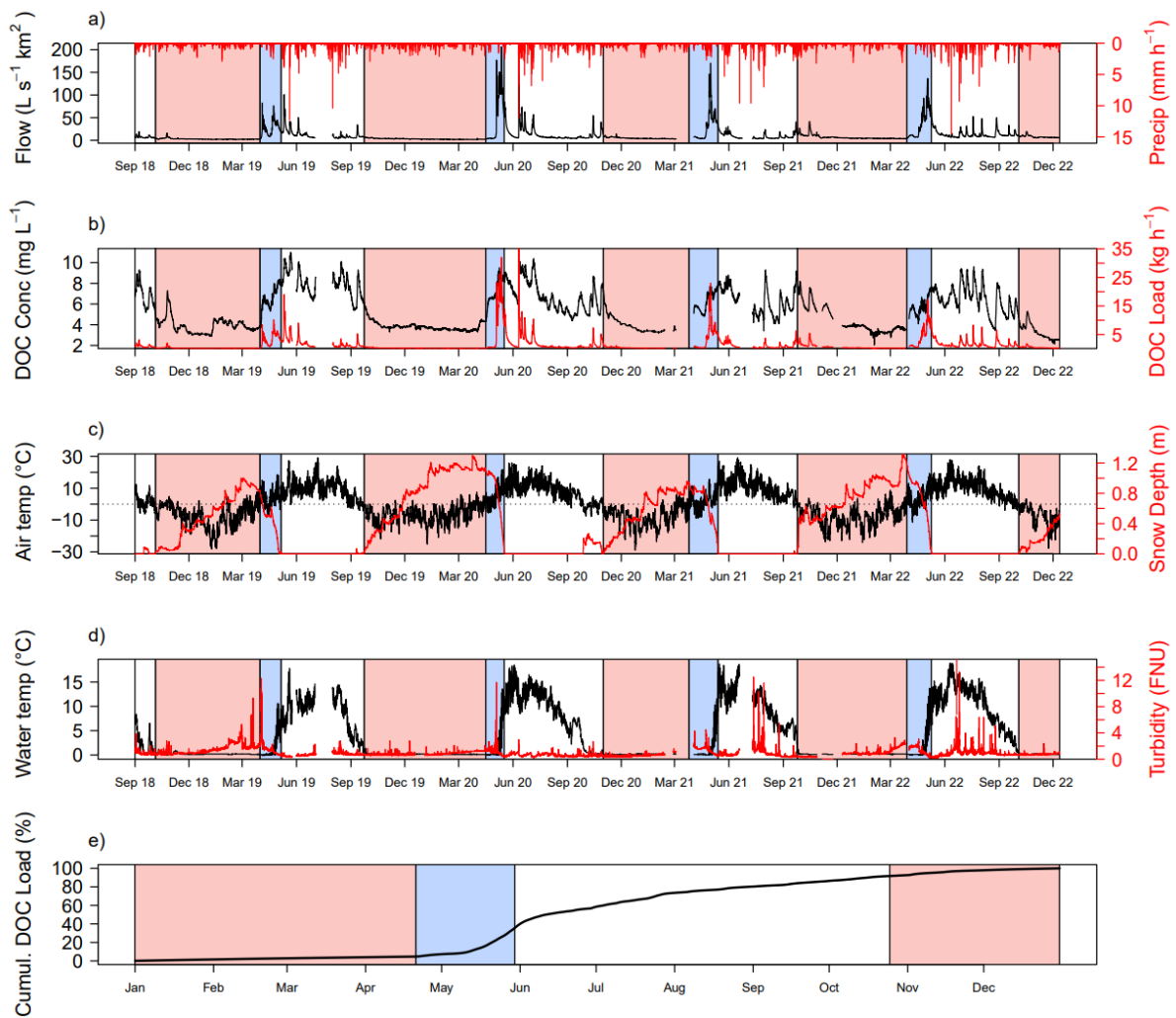
334

335

336

337

338



339

340

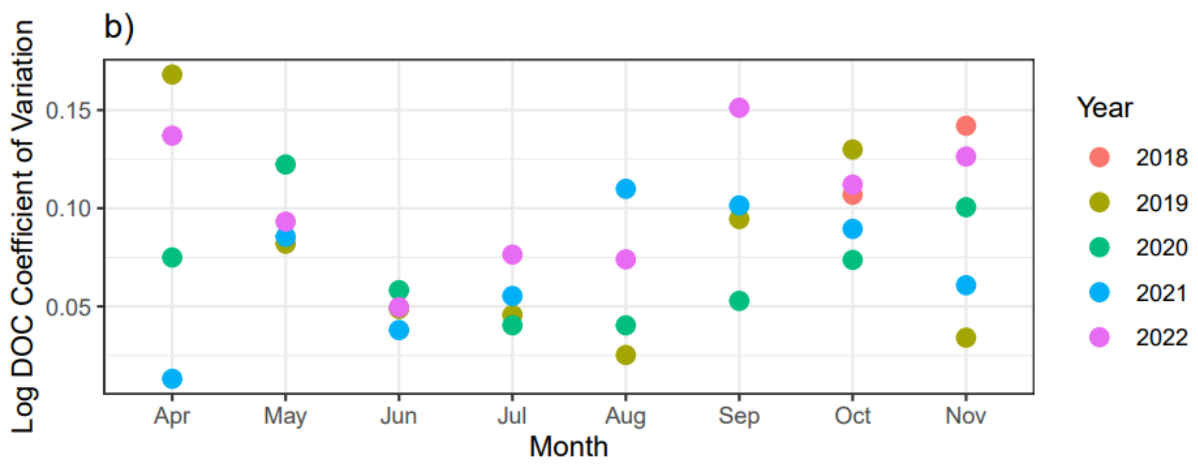
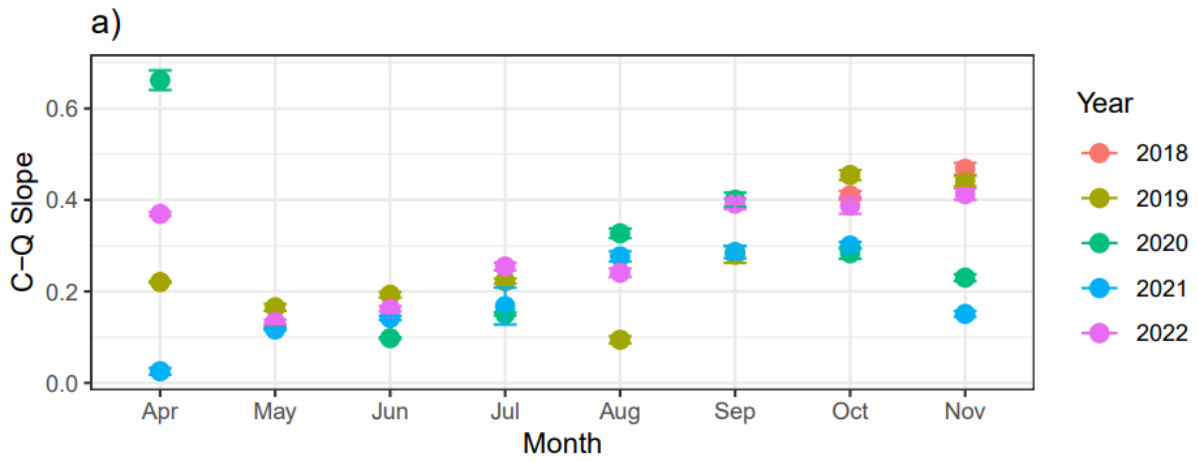
341 **Figure 2** – Time series depicting: a) Flow (black) and Precipitation (red), b) DOC
 342 concentration (black) and DOC load (red), c) Air temperature (black) and snow depth (red),
 343 d) Water temperature (black) and Turbidity (red), and e) Average cumulative DOC load for
 344 the study period. The background shading indicates the different seasons: white background
 345 represents the snow-free season, red background represents the snow cover season, and
 346 blue background represents the snowmelt season. In graph e, the shading represents the
 347 average date of the snow-free, permanent snow cover, and snowmelt seasons.

348 **3.2 Concentration-discharge (C-Q) relationships**

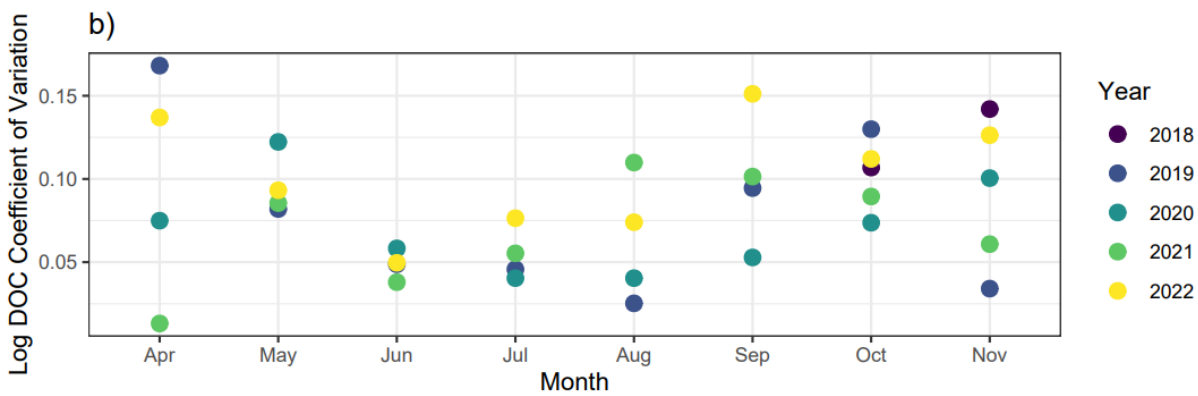
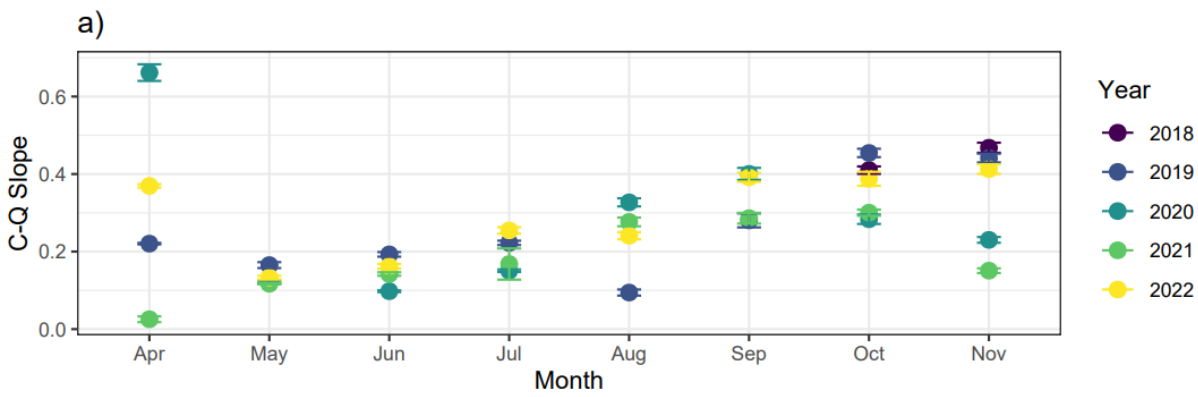
349 The analysis of the C-Q relationship revealed consistent positive slopes across all months
 350 and years, indicating transport limitation (Fig. 3a). A pronounced seasonal trend in slope
 351 was observed throughout the study period. From May to November, the slope exhibited a
 352 consistent increase. In April, substantial variation in slopes was observed, primarily driven
 353 by minimal flow changes in most years. Occasional outliers were noted in August 2019, and
 354 November 2020 and 2021; but these were attributable to minimal range in flow in those

355 months. Notably, the variation between years was relatively small and generally smaller
356 than the month-to-month differences. The coefficient of variance data shows strong
357 seasonal and between years differences in variation of the DOC data (Fig. 3b). The largest
358 variation of DOC between years occurred during April and May, while in the summer
359 months of June to August, variation was continuously the lowest, before subsequently
360 increasing again in the Autumn months.

361 In contrast, when considering events only, the C-Q slope showed less pronounced seasonal
362 variation (Fig. 4a). No significant differences were found between months ($df = 7$, $F = 0.77$, P
363 $\Rightarrow 0.6205$) or seasons ($df = 2$, $F = 1.54$, $P \Rightarrow 0.2205$), although the slope during snow cover
364 exhibited slightly higher values compared to other months. Notably, non-linear relationships
365 emerged between the C-Q slope and 7-day antecedent precipitation for flow events (Fig.
366 4b). During the snow-free season, the slope was significantly negatively correlated with
367 antecedent precipitation up to approximately 20 mm ($R^2 = 0.26$, $P \leq 0.0006001$), beyond
368 which the slope relationship plateaued around 0 despite increasing antecedent
369 precipitation. A similar significant relationship was observed during the snow cover season
370 ($R^2 = 0.57$, $P < 0.0041$). However, a no significant relationship was observed during the
371 snowmelt season ($R^2 = 0.00$, $P = 0.99 > 0.05$). Interestingly, the C-Q slope consistently
372 exhibited higher values during the snow cover season compared to the snow-free season.



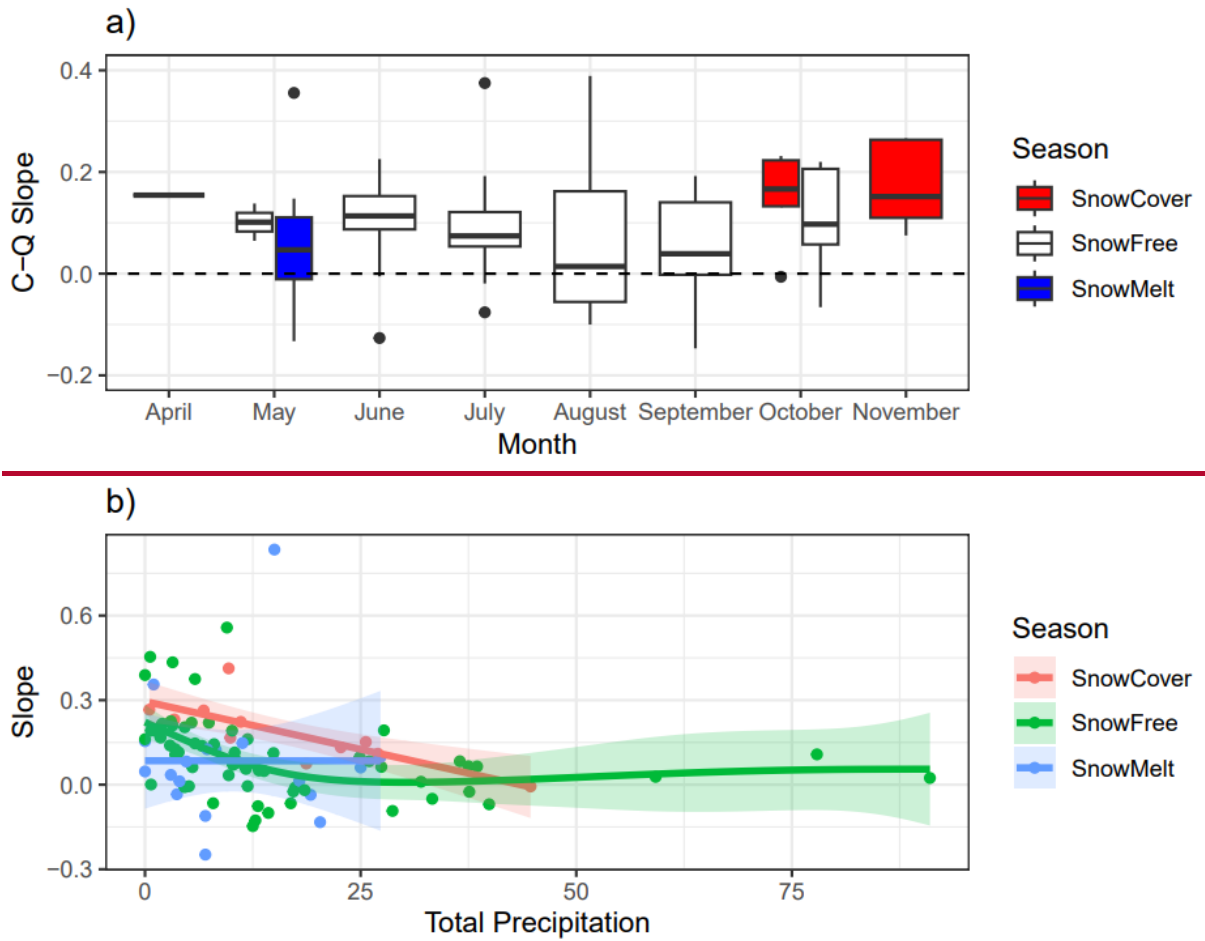
373



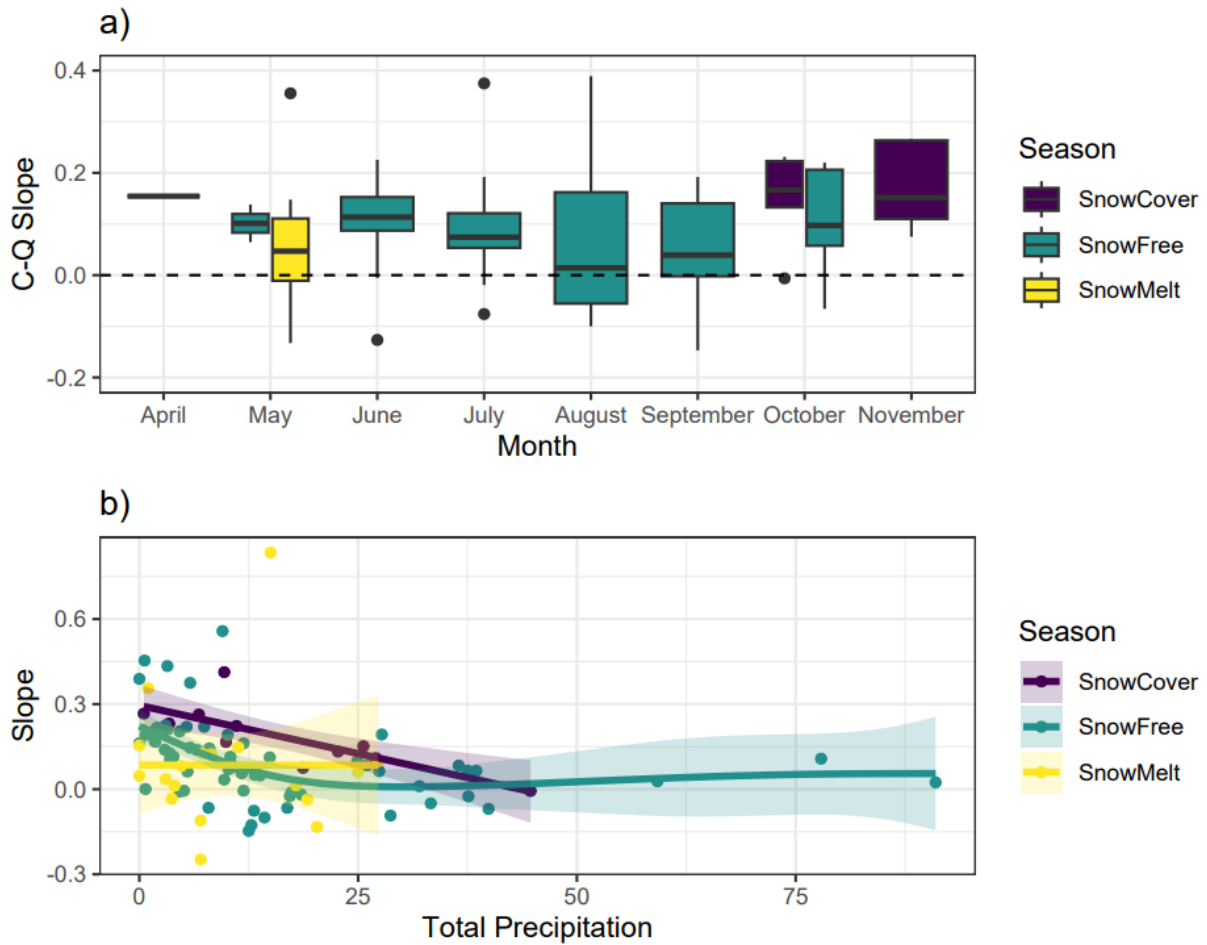
374

375

376 **Figure 3 – a)** All flow C-Q Slope Analysis. Each individual dot represents the slope of the C-Q
377 relationship for the given month. B) All Log DOC coefficient of variation. Each individual dot
378 represents the coefficient of variation for Log DOC for the given month, thus showing the
379 variation in DOC by month. The year of the sample is shown by the colour of the dot.
380



381



382

383

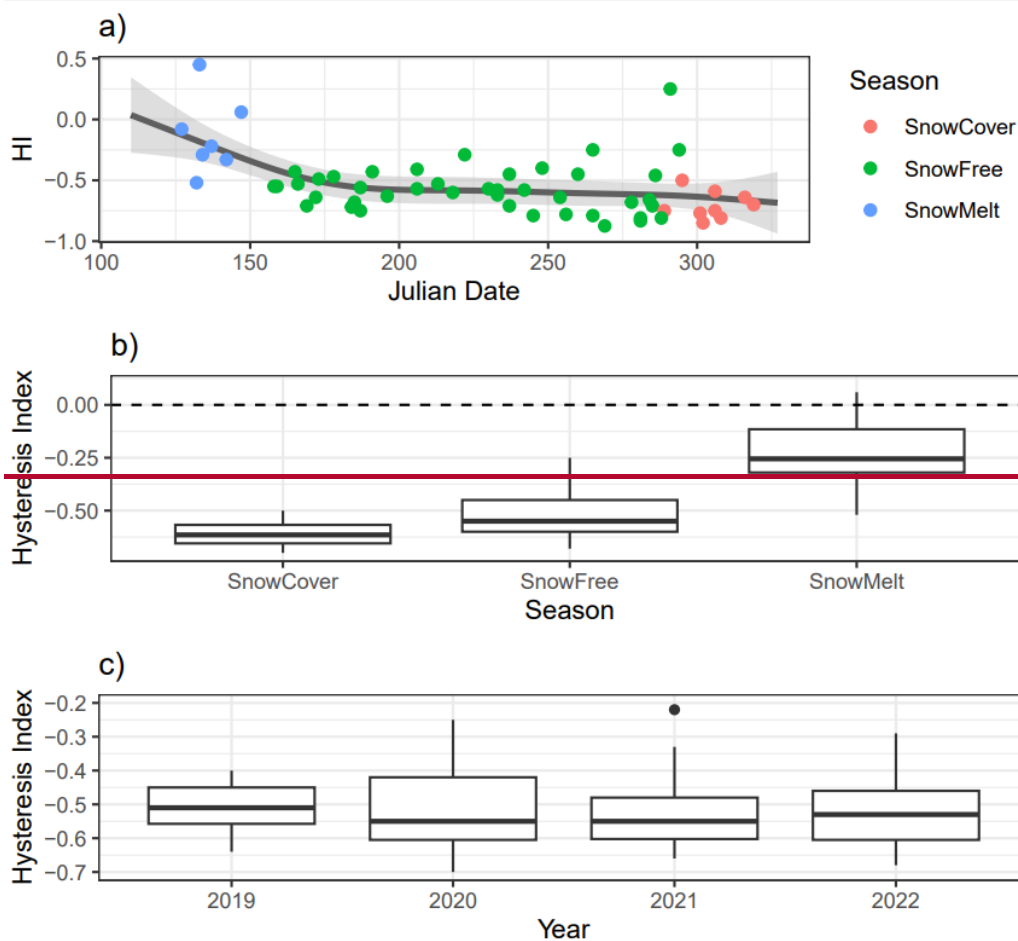
384 **Figure 4** – C-Q slope analysis for individual events. A) Boxplot of C-Q slope for events by
 385 month, b) Relationship of slope of C-Q relationship with 7-day antecedent precipitation.
 386 Shading shows the standard error. Dot colours show season of event, and the line shows the
 387 fitted General Additive Model.

388 **Hysteresis patterns**

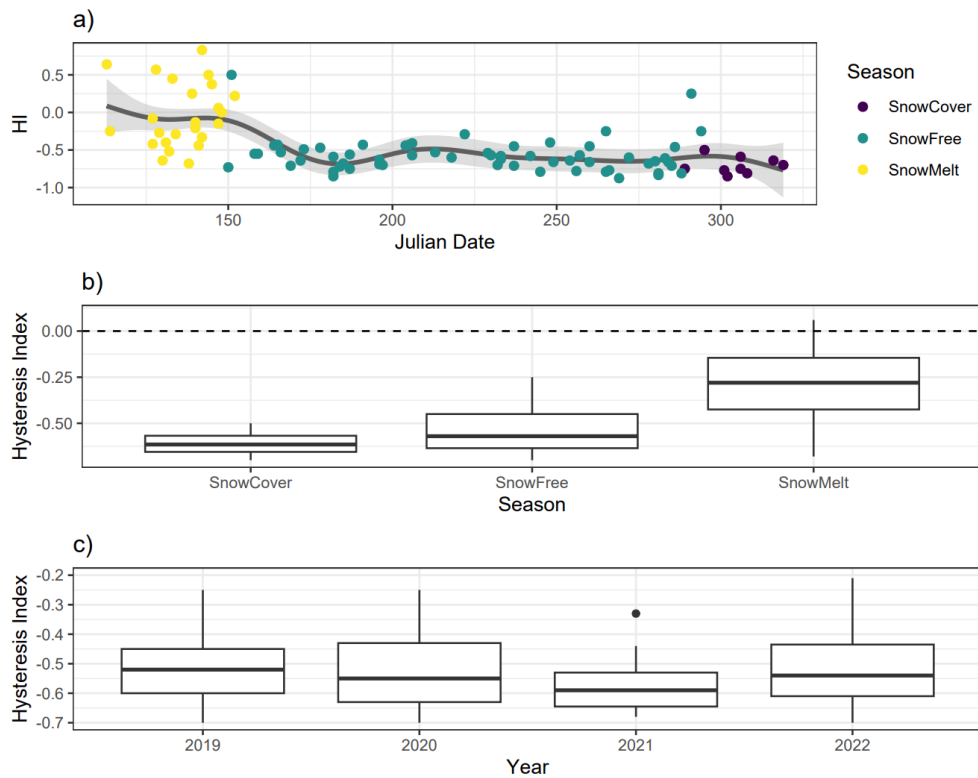
389 In the Hysteresis analysis, the HI exhibited significant ($R^2 = 0.4128$, $P = < 0.00010.001$) and
 390 distinct seasonal patterns (Fig. 5a). During the snowmelt season, HI values were generally
 391 highest, ranging from postive weakly positive to weakly negative. However, as the season
 392 progressed and transitioned into the snow-free season, HI values showed a rapid decline
 393 and remained relatively consistent around -0.5. Throughout the snow cover season, HI
 394 exhibited a relatively stable pattern. Notably, a single positive outlier with an HI value of
 395 0.26 was observed during the snow-free season, which can be attributed to a rare event
 396 characterized by heavy early snowfall followed by subsequent rainfall.

397 Significant differences were found between the snowmelt season and snow free season ($t = 7.75515$, $P < 0.0010001$), and the snowmelt season and snow cover season ($t = 5.9846$, $P < 0.00014$; Fig. 5b), indicating distinct hysteresis patterns during different periods. However, no significant difference was observed between the snow cover season and the snow-free season ($t = 1.3176$, $P = 0.38 > 0.05$), suggesting similar hysteresis behaviour during these periods. Furthermore, there were no significant differences in HI between different years of the study ($df = 4$, $F = 0.8751$, $P = 0.4805$; Fig. 5c), indicating consistent hysteresis patterns across the study duration.

405



406



407

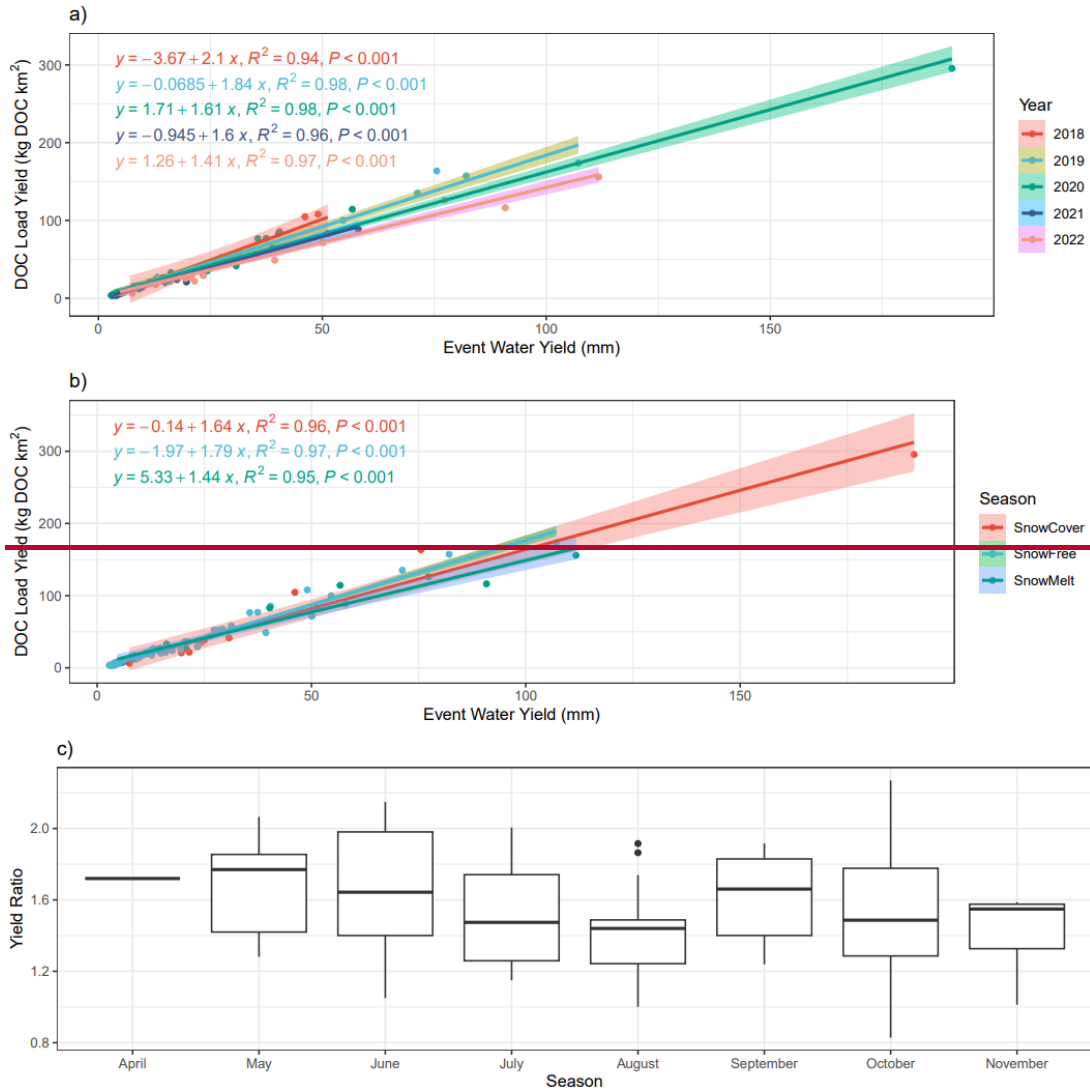
408 **Figure 5** – a) Time series of Hysteresis Index against Julian Date with the fitted general
 409 additive model. Dot colours show seasons. Shading shows the standard error of the
 410 predictions from the general additive model B) Boxplot showing Hysteresis Index variation
 411 by season. C) Boxplot showing Hysteresis Index variation by year.

412 **3.3 DOC load and event water yields relationships**

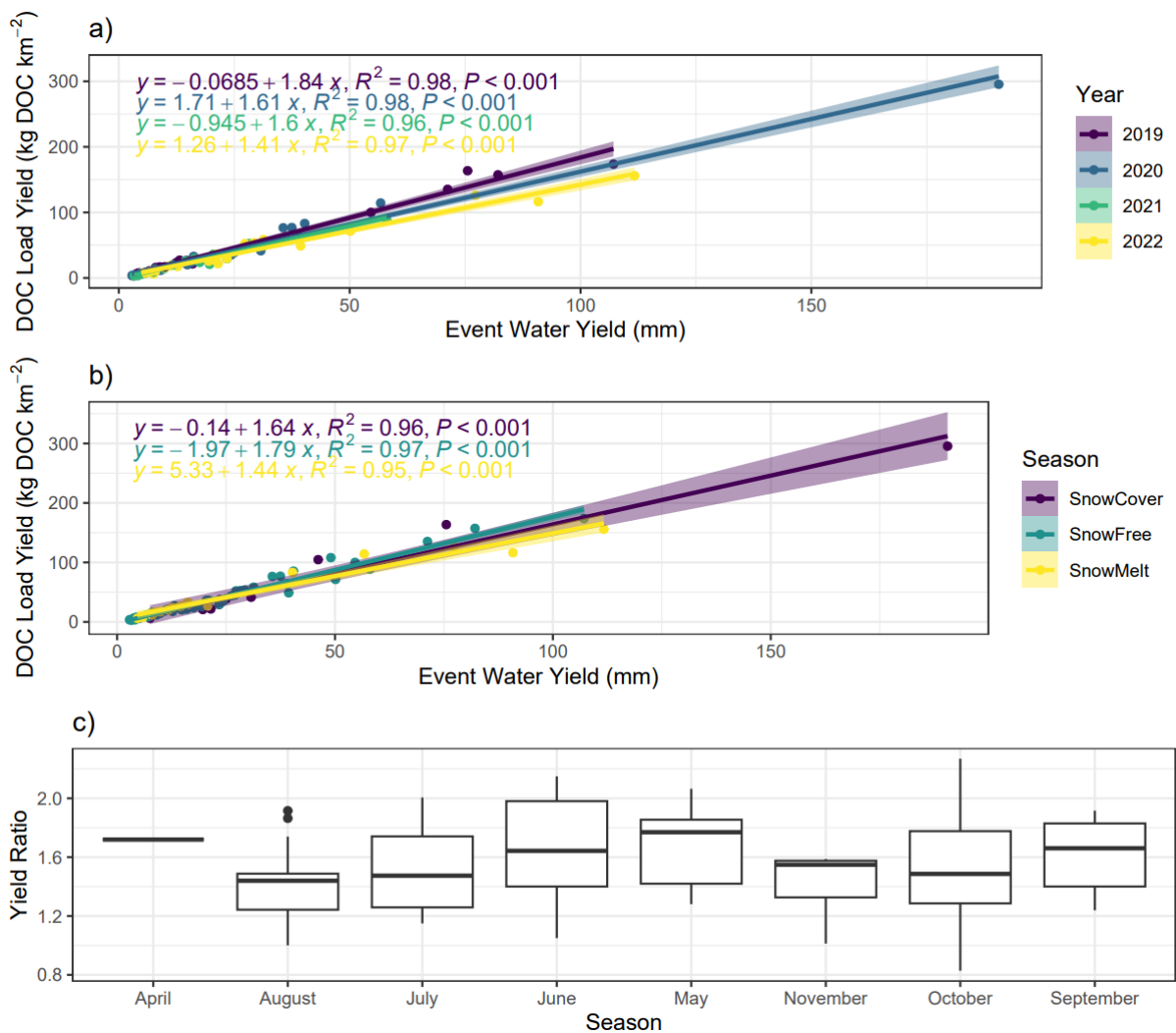
413 The analysis of event yield revealed significant inter-annual variations in the relationship
 414 between DOC load yield and Event Water Yield (Fig. 6a; $df = 3$, $F = 9.70795$, $P < 0.0001$).
 415 Specifically, the regressions for 2018 and for 2019 was significantly steeper than 2020 (~~2018~~
 416 ~~–2020: $T = 3.04$, $P < 0.05$ and 2019 –2020: $t_T = 3.3524$, $P \leq 0.0075$) and 2022 (~~2018 –2022:~~
 417 ~~$T = 4.10$, $P < 0.01$; 2019 –2022: $t_T = 5.3819$, $P \leq 0.0001$), while 2020 was also significantly
 418 steeper than 2022 ($t = 2.77$, $p = 0.035$), indicating differences in the transport and source
 419 dynamics between these years. Additionally, significant differences were observed between
 420 seasons ($df = 2$, $f = 7.13$, $P = 0.001$), where the snowfree season had a significantly higher
 421 regression than the snowmelt season ($t = 3.77$, $P = 0.0008$). However, no significant
 422 differences were observed between the seasons during the study ($F = 0.27$, $P > 0.05$; Fig.
 423 6b).~~~~

424 Across all years and seasons, the relationship between DOC load yield and Event Water Yield
 425 were remained strongly linear (all $P \leq 0.001$; $R^2 = 0.961 - 0.98$). This suggests a consistent

426 and predictable relationship between the amount of ~~DOC dissolved organic carbon~~ and
 427 event water yield. Furthermore, the analysis of the yield ratio across months showed no
 428 apparent seasonal trends (Fig. 6c), with no significant differences observed between months
 429 ($df = 7, F = 1.07; P \Rightarrow 0.3805$).



430



431

432 **Figure 6** – Event yield analysis figures showing a) Linear regression of DOC load yield vs
 433 Event Water Yield separated by year, b) Linear regression of DOC load yield vs Event Water
 434 Yield separated by season, c) Boxplot of yield ratio for different months in study.

435 Additionally, DOC load yield vs event water yield separated by yield only featuring events
 436 with event water yield <50 mm (i.e. removing extreme events) is featured in Supplementary
 437 Figure 2.

438 **3.4 Predictors of Seasonal Variation**

439 During the snowmelt season (Table 2a), the hydrometeorological predictors did not account
 440 for a significant amount of variation. Maximum discharge emerged as the most important
 441 predictor for both the Maximum DOC and C-Q slope models, but the predictive value of
 442 these models was relatively low (19.81% and 10.52% of variance explained, respectively).

443 In contrast, during the snow-free season (Table 2b), the predictors explained a relatively
 444 high amount of variance (55.2%) in the Maximum DOC model, with maximum discharge
 445 identified as the most important predictor (node purity = 50.19). However, for the models of

446 DOC percentage change and yield ratio, 7-day antecedent precipitation was found to be the
 447 most important predictor, although the predictive value of these models was weak (17.68%
 448 and 11.67% of variance explained, respectively).

449 For the snow cover season (Table 2c), maximum discharge remained an important predictor
 450 for the Maximum DOC model. However, for the C-Q slope model, average water
 451 temperature and event rainfall emerged as the strongest predictors. Both the Maximum
 452 DOC and C-Q slope models showed moderate explanatory capability during the snow cover
 453 season, explaining 34.82% and 32.65% of the variance, respectively.

454 **Table 2** – Random Forest regression prediction results for target variables for a) Snow Melt
 455 Events, b) Snow Free Events, and c) Snow Cover Events. The predictor abbreviations are as
 456 follows: MaxDis = Maximum Discharge, AvgWTemp = Average Water Temperature,
 457 AvgATemp = Average Air Temperature, AntPre = 7-day antecedent precipitation, and
 458 EventPre = Total Event Precipitation. The target variables were Maximum DOC value in
 459 events (MaxDOC), the percentage DOC changed from its starting value (DOC Change), the C-
 460 Q slope of events (Slope), the Hysteresis Index (HI), and the Yield Ratio (Yield Ratio). The
 461 value in the predictors column represents the node purity. Additionally, the table presents
 462 the variance explained (%var) and the mean of squared residuals for each model (Res
 463 Mean). NS = Not significant.

a) Snow Melt							
	Predictors					Model	
Target	MaxDis	AvgW Temp	AvgA Temp	AntPre	EventPre	%Var	Res Mean
MaxDOC	3.18	2.80	2.70	2.15	1.06	19.81	0.61
DOC Change						NS	
Slope	0.227	0.14	0.15	0.07	0.04	10.52	0.04
Yield Ratio						NS	
b) Snow Free							
	Predictors					Model	
Target	MaxDis	AvgW Temp	AvgA Temp	AntPre	EventPre	%Var	Res Mean
MaxDOC	50.19	17.45	15.12	21.51	30.21	55.2	1.04
DOC Change	6712.51	5572.31	5767.61	9270.8	6113.33	17.68	523.9
Slope						NS	
Yield Ratio	1.06	0.95	0.92	1.17	0.96	11.67	0.08
c) Snow Cover							
	Predictors					Model	

Target	MaxDis	AvgW Temp	AvgA Temp	AntPre	EventPre	%Var	Res Mean
MaxDOC	1069.83	1035.79	885.8	585.89	531.53	34.82	285.6
DOC Change						NS	
Slope	0.01	0.02	0.01	0.01	0.02	32.55	0.01
Yield Ratio						NS	

464

465 **4.0 Discussion**

466 **4.1 Seasonal Variation in DOC Transport Processes**

467 Distinct seasonal variations were evident in the DOC transport processes, shedding light on
468 their changing characteristics during different periods. Notably, the snowmelt season
469 exhibited the lowest C-Q slope (Fig. 3a), albeit still positive, indicating a relatively lower
470 degree of transport limitation compared to other seasons (Gómez-Gener et al., 2021). This
471 can be attributed to the limited availability of sources during the snowmelt season
472 (Ruckhaus et al., 2023; Shogren et al., 2021). The theory of less source availability during
473 snowmelt is further supported by fact that the regression between snowmelt DOC load yield
474 and event water yield (Fig. 6b) was significantly lower compared to the snow free period.
475 This suggests during snow melt there is less DOC transported per unit of water, possibly
476 reflecting the reduced amount of DOC sources in the snowmelt season compared to the
477 snow free period (Shatilla et al., 2023; Vaughan et al., 2017). -During the snowmelt, isotope
478 separation indicated approximately 60% of the stream water is comprised of event water,
479 i.e., the melting snowpack (Noor et al., 2023)(Noor et al in review). The onset of snowmelt is
480 characterized by more rapid melting in the peatland compared to the hillslopes, while
481 surface pathways dominate and facilitate rapid DOC transport compared to later in the year
482 (Laudon et al., 2004). This observation is further supported by the high (positive) HI values
483 during the snowmelt season, indicating the connectivity of new near-stream sources and
484 the rapid flushing of DOC from the catchment during this period (Croghan et al., 2023;
485 Shatilla et al., 2023)(Croghan et al., 2023). However, when exclusively examining event flows
486 rather than encompassing all flow conditions (Fig. 4a), no significant disparity was observed
487 between snowmelt conditions and other months. In contrast, C-Q slope values exhibited a
488 general reduction across all months, when compared to slope values for all flow conditions.
489 This reduction may suggest that transport limitation reduces, and increased source

490 depletion occurs relatively quickly after flow increases beyond baseflow conditions across all
491 seasons.

492 ~~In contrast, the relationship between snowmelt DOC load yield and event water yield (Fig.~~
493 ~~6b) did not exhibit significant variation compared to other seasons. This (Shatilla et al.,~~
494 ~~2023) suggests that although the transport processes differed, the overall amount of DOC~~
495 ~~relative to the unit of water remained relatively consistent. Thus, despite variations in~~
496 ~~sources and transport mechanisms, a sustained supply of DOC was observed without~~
497 ~~deviating from linearity, implying a readily available reservoir of DOC in the catchment~~
498 ~~during the snowmelt season. This was possibly because of an accumulation of DOC on the~~
499 ~~top soil surface during winter (Billett et al., 2006; Dyson et al., 2011). In Pallas, soil frost is~~
500 ~~relatively minimal in the peatlands and soil temperature remains above zero during early~~
501 ~~winter which allows for the production of DOC (Marttila et al., 2021). Furthermore, in a~~
502 ~~previous study in Pallas, top soil water (up to 1 m) has been noted to be replaced two times~~
503 ~~annually (Muhic et al., 2023) firstly during the snow melt and then secondly during the~~
504 ~~late summer. This also primes conditions for DOC transport from the soil column during~~
505 ~~these periods, supporting our observations from the stream.~~

506 During the snow-free season, the C-Q slopes became consistently more transport-limited as
507 the season progressed (Fig. 3a), likely due to increased source availability as the catchment
508 gradually wetted up, activating pathways and connectivity (Birkel et al., 2017; Gómez-Gener
509 et al., 2021). Additionally, enhanced microbial activity and increased vegetation breakdown
510 throughout the growing season could provide more abundant sources of DOC (Campbell et
511 al., 2022), and may also be an explanatory factor in the higher DOC yield during snow free
512 events compared to the snowmelt period. This interpretation is partially supported by the
513 HI, which consistently revealed strong anti-clockwise hysteresis, indicative of likely distal
514 sources and slow DOC transport (Ducharme et al., 2021). However, the HI did not show
515 significant seasonal variation across the snow-free season. ~~Notably, a steeper linear~~
516 ~~relationship between DOC yield and event yield was observed during the snow-free season~~
517 ~~compared to the snowmelt season (Fig. 6b), suggesting a greater supply of DOC per unit of~~
518 ~~water during events (Vaughan et al., 2017).~~ Furthermore, while maximum discharge
519 consistently influenced DOC dynamics in all seasons, antecedent precipitation emerged as
520 an important predictor during the snowmelt season, highlighting the role of prior rainfall in

521 supporting transport dynamics (Blaen et al., 2017; Tiefenbacher et al., 2021). For the C-Q
522 slope (Fig. 3c), higher antecedent rainfall led to reduced transport limitation, suggesting the
523 exhaustion of certain sources to some extent. Interestingly, the relationship was non-linear,
524 and with high antecedent rainfall, no further change in the relationship was observed,
525 possibly indicating that high antecedent rainfall enables the transport of new sources of
526 DOC, preventing the system from becoming source limited, even under extremely high
527 antecedent precipitation or large events.

528 Surprisingly, the snow cover season (late October, November) exhibited the highest values
529 for the C-Q slope, indicating that increasing source limitation did not occur despite the
530 presence of snow cover (Fig. 3A), possibly ~~resultant from~~ due to the decay of organic matter
531 providing a large source of DOC ~~dominating~~ after the end of the growing season.

532 Interestingly, the C-Q slope was also consistently higher with antecedent rainfall during the
533 snow cover season, compared to the snow free season. This suggests that antecedent
534 rainfall had a lesser impact on reducing source supply during this period. The antecedent
535 rainfall may also come as snow, and the snowmelt vs rainfall contribution to discharge in the
536 early snow season are difficult to identify. One possible explanation is that the snow cover
537 season begins in the hills and forests, where the snow depth is recorded (Kenttäröva station
538 Fig. 1), while the snow cover on the peatland occurs later (Croghan et al., 2023; Marttila et
539 al., 2021). Consequently, during the snow cover season, the hillslopes, which likely
540 contribute less carbon per unit of water, are cut off, while the carbon-enriched peatlands
541 make an increased contribution to streamflow during events compared to other seasons
542 (Gómez-Gener et al., 2021; Rosset et al., 2019). However, neither the HI nor yield analysis
543 showed significant variation during the snow cover season. The use of spatially distributed
544 hydrological models in future studies would be valuable in identifying source contributors
545 and further investigating if the differences in source contributions during the snow cover
546 season drive the observed variations in C-Q relationships (Ala-aho et al., 2018; Birkel et al.,
547 2017).

548 **4.2 Inter-Annual Variation in Transport Processes**

549 Despite significant year-to-year variations in hydrometeorological conditions, including
550 snow cover onset and snowmelt conditions, we found limited inter-annual variation in the
551 C-Q slope and HI (Fig. 3-5), However, exceptions were noted in the shoulder months of April

552 and November, where variations in inter-annual transport metric values stemmed from the
553 fact that, in certain years, minimal flow variation occurred due to the catchment remaining
554 in frozen conditions, whereas in other years, large events occurred during these months.
555 While there were some differences in C-Q slopes between years, the month-to-month
556 variation generally outweighed the year-to-year ~~variation~~, suggesting a remarkable
557 consistency in the degree of seasonality in transport limitation throughout the study. This
558 consistency implies activation of consistent sources and flow pathways from year to year
559 (Vaughan et al., 2017; Zarnetske et al., 2018; Shatilla et al., 2023)~~(Vaughan et al., 2017;~~
560 ~~Zarnetske et al., 2018)~~. Similarly, the HI values showed no discernible differences on an annual
561 basis, indicating flow path stability in this system (Lloyd et al., 2016b). Source activation and
562 transport processes have a strong seasonal pattern; however, the differences between
563 years may not have been pronounced enough to drive substantial changes, underscoring
564 the need for longer-term data series for a comprehensive understanding.

565 In contrast, the yield analysis revealed variations between years. Specifically, we observed
566 steeper regressions for ~~2018 and~~ 2019 compared to 2020 and 2022, and for 2020 relative to
567 2022, indicating a higher transport of DOC per unit of water during these years, however
568 when extreme events were removed from the analysis (Supplementary Figure 2),
569 differences between the years disappeared. Thus, ~~though source activation processes do~~
570 ~~not appear to be changing year on year, the~~ the relationship between DOC yield and event
571 water yield appears to be consistent between years ~~does, which highlights the need to~~
572 ~~understand how changes in water source contribution drive changes in both processes and~~
573 ~~yield~~ with differences between years driven by differences in the extent of annual extreme
574 events. While ~~p~~ Previous long-term studies have suggested that warmer years lead to
575 increased mobilization of DOC, possibly due to reduced snowpack duration which creates
576 more potential for soil C to be mobilised and a greater potential breakdown of the humic
577 layer (Bowering et al., 2023, 2020), we did not find notable differences between years for
578 the amount of mobilization of DOC per unit of water, suggesting a strong consistency
579 between the amount of DOC produced year on year, despite differing climatic conditions.
580 Possibly this is because although there were climatic differences between years, they were
581 not strong enough to drive differences in DOC production. Differences were instead driven
582 by the extent of extreme events, thus the expected increase in occurrence and magnitude

583 of extreme rainfall events in the Arctic is likely to be a substantial driver of differences in
584 DOC mobilization in the future (Beel et al., 2021; McCrystall et al., 2021). ~~Although 2019~~
585 ~~was not an exceptionally warmer year, we did observe a quicker onset of snowmelt peaks~~
586 ~~(Croghan et al., 2023). Consequently, years with rapid snowmelt onset may result in a~~
587 ~~greater mobilization of DOC per unit of water.~~ In the longer term, differences in annual
588 trends may be more apparent as the warming climate will also impact vegetation and
589 peatland formation patterns (Sallinen et al., 2023), which eventually impact also flow paths,
590 connectivity and DOC transport. Thus, highlighting the need to maintain critical
591 environmental monitoring infrastructure in high latitudes.

592 **5.0 Conclusions**

593 Our study provides valuable insights into the seasonal and inter-annual variations in DOC
594 transport processes in the Arctic, stressing the need for comprehensive monitoring across
595 all seasons. By examining various transport metrics, we observed distinct patterns that
596 enhance our understanding of carbon dynamics in Arctic ecosystems. The observed seasonal
597 variations in C-Q slopes indicate a progressive increase in transport limitation as the year
598 progresses from snowmelt to snow-free season to snow-covered season due to increased
599 source supply. The decline in hysteresis index after the snowmelt season highlights the rapid
600 flushing of DOC from the catchment during this period. ~~Importantly, the relationship~~
601 ~~between DOC yield and event water yield remained consistent across seasons, suggesting a~~
602 ~~stable supply of DOC per unit of water.~~ However, high-resolution DOC monitoring is needed
603 ~~for improving to unravel seasonal variability in~~ DOC storage and transport process and
604 responses to extreme events understanding. Interestingly, despite significant year-to-year
605 variations in hydrometeorological conditions, the intra-annual variation in transport
606 processes was relatively low. This suggests a remarkable consistency in the activation and
607 deactivation of sources and flow pathways over the study period. However, longer-term
608 records are necessary to fully comprehend the impacts of climate change on DOC transport
609 processes as headwater are anticipated to warm and experienced greater and more regular
610 extreme events, which will cause shifts in water sources and paths ~~shift~~.

611 Our findings emphasize the ~~vulnerability-sensitivity~~ of DOC transport processes to change
612 with changing snow and snowmelt season ality in response to climate change. Our study
613 highlights the importance of long-term monitoring to assess the long-term impacts on DOC

614 transport. To further enhance our understanding, future research should focus on better
615 understanding how DOM compositional changes impact DOC fate in headwater catchments,
616 establishing and establishing causal relationships between transport metrics, in-stream
617 processing and empirical indicators of sources and transport processes pathways. A
618 promising avenue for further research involves, integrating high-resolution stable water
619 isotope monitoring and spatially distributed hydrological modelling with *in-situ* DOC
620 monitoring of quantity and quality (e.g. combined fluorescence and absorbance
621 measurements)g. -This work contributes to advancing our knowledge of DOC transport
622 processes in Arctic ecosystems, providing valuable information for informed decision-
623 making and effective management of these fragile environments in the face of climate
624 change.

625 **Data Availability**

626 Data supporting this study are available from the corresponding author upon request.

627 **Author Contribution**

628 Conceptualization: DC, HM, PAA, KK, DMH. Formal Analysis: DC, Funding Acquisition: HM,
629 JW, BK, Investigation: DC, Resources: HM, BK, JW, JV, Visualization: DC, Writing – original
630 draft preparation: DC, Writing – review & editing: DC, PAA, JW, KRM, KK, DMH, JV, BK, HM.

631 **Competing Interests**

632 The authors declare that they have no conflict of interest.

633 **Acknowledgements**

634 The study was supported by the Maa-ja Vesitekniiikan Tuki ry, the K. H. Renlund Foundation,
635 the Academy of Finland (projects: 316349, 316014, 308511, 318930, 312559, and 337552),
636 the Strategic Research Council, JMW's UArctic Research Chairship, and the University of
637 Oulu Kvantum Institute. The study is part of the activities of the National Freshwater
638 Competence Centre (FWCC).

639

640 **References**

641 Ala-aho, P., Soulsby, C., Pokrovsky, O. S., Kirpotin, S. N., Karlsson, J., Serikova, S., Vorobyev, S. N.,
642 Manasypov, R. M., Loiko, S., and Tetzlaff, D.: Using stable isotopes to assess surface water source
643 dynamics and hydrological connectivity in a high-latitude wetland and permafrost influenced
644 landscape, *Journal of Hydrology*, 556, 279–293, <https://doi.org/10.1016/J.JHYDROL.2017.11.024>,
645 2018.

646 Anderson, L. E., DeMont, I., Dunnington, D. D., Bjorndahl, P., Redden, D. J., Brophy, M. J., and
647 Gagnon, G. A.: A review of long-term change in surface water natural organic matter concentration
648 in the northern hemisphere and the implications for drinking water treatment, *Science of The Total*
649 *Environment*, 858, 159699, <https://doi.org/10.1016/j.scitotenv.2022.159699>, 2023.

650 Argerich, A., Haggerty, R., Johnson, S. L., Wondzell, S. M., Dosch, N., Corson-Rikert, H., Ashkenas, L.
651 R., Pennington, R., and Thomas, C. K.: Comprehensive multiyear carbon budget of a temperate
652 headwater stream, *Journal of Geophysical Research: Biogeosciences*, 121, 1306–1315,
653 <https://doi.org/10.1002/2015JG003050>, 2016.

654 Beel, C. R., Heslop, J. K., Orwin, J. F., Pope, M. A., Schevers, A. J., Hung, J. K. Y., Lafrenière, M. J., and
655 Lamoureux, S. F.: Emerging dominance of summer rainfall driving High Arctic terrestrial-aquatic
656 connectivity, *Nature Communications*, 12, 1–9, <https://doi.org/10.1038/s41467-021-21759-3>, 2021.

657 Billett, M. F., Deacon, C. M., Palmer, S. M., Dawson, J. J. C., and Hope, D.: Connecting organic carbon
658 in stream water and soils in a peatland catchment, *Journal of Geophysical Research: Biogeosciences*,
659 111, <https://doi.org/10.1029/2005JG000065>, 2006.

660 Bintanja, R. and Andry, O.: Towards a rain-dominated Arctic, *Nature Climate Change*, 7, 263–267,
661 <https://doi.org/10.1038/nclimate3240>, 2017.

662 Birkel, C., Broder, T., and Biester, H.: Nonlinear and threshold-dominated runoff generation controls
663 DOC export in a small peat catchment, *Journal of Geophysical Research: Biogeosciences*, 122, 498–
664 513, <https://doi.org/10.1002/2016JG003621>, 2017.

665 Blaen, P. J., Khamis, K., Lloyd, C. E. M., Bradley, C., Hannah, D., and Krause, S.: Real-time monitoring
666 of nutrients and dissolved organic matter in rivers: Capturing event dynamics, technological
667 opportunities and future directions, *Science of The Total Environment*, 569–570, 647–660,
668 <https://doi.org/10.1016/J.SCITOTENV.2016.06.116>, 2016.

669 Blaen, P. J., Khamis, K., Lloyd, C., Comer-Warner, S., Ciocca, F., Thomas, R. M., MacKenzie, A. R., and
670 Krause, S.: High-frequency monitoring of catchment nutrient exports reveals highly variable storm
671 event responses and dynamic source zone activation, *Journal of Geophysical Research:*
672 *Biogeosciences*, 122, 2265–2281, <https://doi.org/10.1002/2017JG003904>, 2017.

673 Bokhorst, S., Pedersen, S. H., Brucker, L., Anisimov, O., Bjerke, J. W., Brown, R. D., Ehrich, D., Essery,
674 R. L. H., Heilig, A., Ingvander, S., Johansson, C., Johansson, M., Jónsdóttir, I. S., Inga, N., Luojus, K.,
675 Macelloni, G., Mariash, H., McLennan, D., Rosqvist, G. N., Sato, A., Savela, H., Schneebeli, M.,
676 Sokolov, A., Sokratov, S. A., Terzago, S., Vikhamar-Schuler, D., Williamson, S., Qiu, Y., and Callaghan,
677 T. V.: Changing Arctic snow cover: A review of recent developments and assessment of future needs
678 for observations, modelling, and impacts, *Ambio*, 45, 516–537, <https://doi.org/10.1007/s13280-016-0770-0>, 2016.

680 Bowering, K. L., Edwards, K. A., Prestegard, K., Zhu, X., and Ziegler, S. E.: Dissolved organic carbon
681 mobilized from organic horizons of mature and harvested black spruce plots in a mesic boreal
682 region, *Biogeosciences*, 17, 581–595, <https://doi.org/10.5194/bg-17-581-2020>, 2020.

683 Bowering, K. L., Edwards, K. A., Wiersma, Y. F., Billings, S. A., Warren, J., Skinner, A., and Ziegler, S. E.:
684 Dissolved Organic Carbon Mobilization Across a Climate Transect of Mesic Boreal Forests Is
685 Explained by Air Temperature and Snowpack Duration, *Ecosystems*, 26, 55–71,
686 <https://doi.org/10.1007/s10021-022-00741-0>, 2023.

687 Bring, A., Fedorova, I., Dibike, Y., Hinzman, L., Mård, J., Mernild, S. H., Prowse, T., Semanova, O.,
688 Stuefer, S. L., and Woo, M.-K.: Arctic terrestrial hydrology: A synthesis of processes, regional effects,
689 and research challenges, *Journal of Geophysical Research: Biogeosciences*, 121, 621–649,
690 <https://doi.org/10.1002/2015JG003131>, 2016.

691 Bruhwiler, L., Parmentier, F. J. W., Crill, P., Leonard, M., and Palmer, P. I.: The Arctic Carbon Cycle
692 and Its Response to Changing Climate, *Current Climate Change Reports*, 7, 14–34,
693 <https://doi.org/10.1007/s40641-020-00169-5>, 2021.

694 Campbell, T. P., Ulrich, D. E. M., Toyoda, J., Thompson, J., Munsky, B., Albright, M. B. N., Bailey, V. L.,
695 Tffailly, M. M., and Dunbar, J.: Microbial Communities Influence Soil Dissolved Organic Carbon
696 Concentration by Altering Metabolite Composition, *Frontiers in Microbiology*, 12, 2022.

697 Campeau, A. and del Giorgio, P. A.: Patterns in CH₄ and CO₂ concentrations across boreal rivers:
698 Major drivers and implications for fluvial greenhouse emissions under climate change scenarios,
699 *Global Change Biology*, 20, 1075–1088, <https://doi.org/10.1111/gcb.12479>, 2014.

700 Croghan, D., Ala-Aho, P., Lohila, A., Welker, J., Vuorenmaa, J., Kløve, B., Mustonen, K.-R., Aurela, M.,
701 and Marttila, H.: Coupling of Water-Carbon Interactions During Snowmelt in an Arctic Finland
702 Catchment, *Water Resources Research*, 59, e2022WR032892,
703 <https://doi.org/10.1029/2022WR032892>, 2023.

704 Csank, A. Z., Czimeczik, C. I., Xu, X., and Welker, J. M.: Seasonal Patterns of Riverine Carbon Sources
705 and Export in NW Greenland, *Journal of Geophysical Research: Biogeosciences*, 124, 840–856,
706 <https://doi.org/10.1029/2018JG004895>, 2019.

707 Day, J. J. and Hodges, K. I.: Growing Land-Sea Temperature Contrast and the Intensification of Arctic
708 Cyclones, *Geophysical Research Letters*, 45, 3673–3681, <https://doi.org/10.1029/2018GL077587>,
709 2018.

710 Dick, J. J., Tetzlaff, D., Birkel, C., and Soulsby, C.: Modelling landscape controls on dissolved organic
711 carbon sources and fluxes to streams, *Biogeochemistry*, 122, 361–374,
712 <https://doi.org/10.1007/s10533-014-0046-3>, 2015.

713 Downing, B. D., Pellerin, B. A., Bergamaschi, B. A., Saraceno, J. F., and Kraus, T. E. C.: Seeing the light:
714 The effects of particles, dissolved materials, and temperature on in situ measurements of DOM
715 fluorescence in rivers and streams, *Limnology and Oceanography: Methods*, 10, 767–775,
716 <https://doi.org/10.4319/lom.2012.10.767>, 2012.

717 Ducharme, A. A., Casson, N. J., Higgins, S. N., and Friesen-Hughes, K.: Hydrological and catchment
718 controls on event-scale dissolved organic carbon dynamics in boreal headwater streams,
719 *Hydrological Processes*, 35, e14279, <https://doi.org/10.1002/HYP.14279>, 2021.

720 Dyson, K. E., Billett, M. F., Dinsmore, K. J., Harvey, F., Thomson, A. M., Piirainen, S., and Kortelainen,
721 P.: Release of aquatic carbon from two peatland catchments in E. Finland during the spring
722 snowmelt period, *Biogeochemistry*, 103, 125–142, <https://doi.org/10.1007/s10533-010-9452-3>,
723 2011.

724 Finlay, J., Neff, J., Zimov, S., Davydova, A., and Davydov, S.: Snowmelt dominance of dissolved
725 organic carbon in high-latitude watersheds: Implications for characterization and flux of river DOC,
726 *Geophysical Research Letters*, 33, <https://doi.org/10.1029/2006GL025754>, 2006.

- 727 Fork, M. L., Sponseller, R. A., and Laudon, H.: Changing Source-Transport Dynamics Drive Differential
728 Browning Trends in a Boreal Stream Network, *Water Resources Research*, 56, e2019WR026336,
729 <https://doi.org/10.1029/2019WR026336>, 2020.
- 730 Godsey, S. E., Kirchner, J. W., and Clow, D. W.: Concentration-discharge relationships reflect
731 chemostatic characteristics of US catchments, *Hydrological Processes*, 23, 1844–1864,
732 <https://doi.org/10.1002/hyp.7315>, 2009.
- 733 Gómez-Gener, L., Hotchkiss, E. R., Laudon, H., and Sponseller, R. A.: Integrating Discharge-
734 Concentration Dynamics Across Carbon Forms in a Boreal Landscape, *Water Resources Research*, 57,
735 e2020WR028806, <https://doi.org/10.1029/2020WR028806>, 2021.
- 736 Koch, J. C., Sjöberg, Y., O'Donnell, J. A., Carey, M. P., Sullivan, P. F., and Terskaia, A.: Sensitivity of
737 headwater streamflow to thawing permafrost and vegetation change in a warming Arctic, *Environ.*
738 *Res. Lett.*, 17, 044074, <https://doi.org/10.1088/1748-9326/ac5f2d>, 2022.
- 739 Lambert, T., Pierson-Wickmann, A.-C., Gruau, G., Jaffrezic, A., Petitjean, P., Thibault, J. N., and
740 Jeanneau, L.: DOC sources and DOC transport pathways in a small headwater catchment as revealed
741 by carbon isotope fluctuation during storm events, *Biogeosciences*, 11, 3043–3056,
742 <https://doi.org/10.5194/bg-11-3043-2014>, 2014.
- 743 Laudon, H., Köhler, S., and Buffam, I.: Seasonal TOC export from seven boreal catchments in
744 northern Sweden, *Aquat. Sci.*, 66, 223–230, <https://doi.org/10.1007/s00027-004-0700-2>, 2004.
- 745 Laudon, H., Berggren, M., Ågren, A., Buffam, I., Bishop, K., Grabs, T., Jansson, M., and Köhler, S.:
746 Patterns and Dynamics of Dissolved Organic Carbon (DOC) in Boreal Streams: The Role of Processes,
747 Connectivity, and Scaling, *Ecosystems*, 14, 880–893, <https://doi.org/10.1007/s10021-011-9452-8>,
748 2011.
- 749 Laudon, H., Spence, C., Buttle, J., Carey, S. K., McDonnell, J. J., McNamara, J. P., Soulsby, C., and
750 Tetzlaff, D.: Save northern high-latitude catchments, *Nature Geoscience*, 10, 324–325,
751 <https://doi.org/10.1038/ngeo2947>, 2017.
- 752 Li, M., Peng, C., Zhang, K., Xu, L., Wang, J., Yang, Y., Li, P., Liu, Z., and He, N.: Headwater stream
753 ecosystem: an important source of greenhouse gases to the atmosphere, *Water Research*, 190,
754 116738, <https://doi.org/10.1016/J.WATRES.2020.116738>, 2021.
- 755 Liu, S., Wang, P., Huang, Q., Yu, J., Pozdniakov, S. P., and Kazak, E. S.: Seasonal and spatial variations
756 in riverine DOC exports in permafrost-dominated Arctic river basins, *Journal of Hydrology*, 612,
757 128060, <https://doi.org/10.1016/j.jhydrol.2022.128060>, 2022.
- 758 Lloyd, C. E. M., Freer, J. E., Johnes, P. J., and Collins, A. L.: Technical Note: Testing an improved index
759 for analysing storm discharge-concentration hysteresis, *Hydrol. Earth Syst. Sci*, 20, 625–632,
760 <https://doi.org/10.5194/hess-20-625-2016>, 2016a.
- 761 Lloyd, C. E. M., Freer, J. E., Johnes, P. J., and Collins, A. L.: Using hysteresis analysis of high-resolution
762 water quality monitoring data, including uncertainty, to infer controls on nutrient and sediment
763 transfer in catchments, *Science of The Total Environment*, 543, 388–404,
764 <https://doi.org/10.1016/J.SCITOTENV.2015.11.028>, 2016b.
- 765 Marttila, H., Lohila, A., Ala-Aho, P., Noor, K., Welker, J. M., Croghan, D., Mustonen, K., Meriö, L.-J.,
766 Autio, A., Muhic, F., Bailey, H., Aurela, M., Vuorenmaa, J., Penttilä, T., Hyöky, V., Klein, E., Kuzmin, A.,
767 Korpelainen, P., Kumpula, T., Rauhala, A., and Kløve, B.: Subarctic catchment water storage and

- 768 carbon cycling – leading the way for future studies using integrated datasets at Pallas, Finland,
769 Hydrological Processes, <https://doi.org/10.1002/HYP.14350>, 2021.
- 770 Marttila, H., Laudon, H., Tallaksen, L. M., Jaramillo, F., Alfredsen, K., Ronkanen, A.-K., Kronvang, B.,
771 Lotsari, E., Kämäri, M., Ala-Aho, P., Nousu, J., Silander, J., Koivusalo, H., and Kløve, B.: Nordic
772 hydrological frontier in the 21st century, *Hydrology Research*, 53, 700–715,
773 <https://doi.org/10.2166/nh.2022.120>, 2022.
- 774 McCrystall, M. R., Stroeve, J., Serreze, M., Forbes, B. C., and Screen, J. A.: New climate models reveal
775 faster and larger increases in Arctic precipitation than previously projected, *Nat Commun*, 12, 6765,
776 <https://doi.org/10.1038/s41467-021-27031-y>, 2021.
- 777 Mcguire, A. D., Anderson, L. G., Christensen, T. R., Scott, D., Laodong, G., Hayes, D. J., Martin, H.,
778 Lorenson, T. D., Macdonald, R. W., and Nigal, R.: Sensitivity of the carbon cycle in the Arctic to
779 climate change, *Ecological Monographs*, 79, 523–555, <https://doi.org/10.1890/08-2025.1>, 2009.
- 780 McGuire, A. D., Lawrence, D. M., Koven, C., Klein, J. S., Burke, E., Chen, G., Jafarov, E., MacDougall, A.
781 H., Marchenko, S., Nicolsky, D., Peng, S., Rinke, A., Ciais, P., Gouttevin, I., Hayes, D. J., Ji, D., Krinner,
782 G., Moore, J. C., Romanovsky, V., Schädel, C., Schaefer, K., Schuur, E. A. G., and Zhuang, Q.:
783 Dependence of the evolution of carbon dynamics in the northern permafrost region on the
784 trajectory of climate change, *Proceedings of the National Academy of Sciences of the United States*
785 *of America*, 115, 3882–3887, <https://doi.org/10.1073/pnas.1719903115>, 2018.
- 786 Metcalfe, D. B., Hermans, T. D. G., Ahlstrand, J., Becker, M., Berggren, M., Björk, R. G., Björkman, M.
787 P., Blok, D., Chaudhary, N., Chisholm, C., Classen, A. T., Hasselquist, N. J., Jonsson, M., Kristensen, J.
788 A., Kumordzi, B. B., Lee, H., Mayor, J. R., Prevéy, J., Pantazatou, K., Rousk, J., Sponseller, R. A.,
789 Sundqvist, M. K., Tang, J., Uddling, J., Wallin, G., Zhang, W., Ahlström, A., Tenenbaum, D. E., and
790 Abdi, A. M.: Patchy field sampling biases understanding of climate change impacts across the Arctic,
791 *Nature Ecology and Evolution*, 2, 1443–1448, <https://doi.org/10.1038/s41559-018-0612-5>, 2018.
- 792 Noor, K., Marttila, H., Welker, J. M., Mustonen, K.-R., Kløve, B., and Ala-aho, P.: Snow sampling
793 strategy can bias estimation of meltwater fractions in isotope hydrograph separation, *Journal of*
794 *Hydrology*, 627, 130429, <https://doi.org/10.1016/j.jhydrol.2023.130429>, 2023.
- 795 Osuch, M., Wawrzyniak, T., and Majerska, M.: Changes in hydrological regime in High Arctic non-
796 glaciated catchment in 1979–2020 using a multimodel approach, *Advances in Climate Change*
797 *Research*, 13, 517–530, <https://doi.org/10.1016/j.accre.2022.05.001>, 2022.
- 798 Pearson, R. G., Phillips, S. J., Loranty, M. M., Beck, P. S. A., Damoulas, T., Knight, S. J., and Goetz, S. J.:
799 Shifts in Arctic vegetation and associated feedbacks under climate change, *Nature Climate Change*,
800 3, 673–677, <https://doi.org/10.1038/nclimate1858>, 2013.
- 801 Pedron, S. A., Jespersen, R. G., Xu, X., Khazindar, Y., Welker, J. M., and Czimczik, C. I.: More Snow
802 Accelerates Legacy Carbon Emissions From Arctic Permafrost, *AGU Advances*, 4, e2023AV000942,
803 <https://doi.org/10.1029/2023AV000942>, 2023.
- 804 Prokushkin, A. S., Pokrovsky, O. S., Shirokova, L. S., Korets, M. A., Viers, J., Prokushkin, S. G., Amon, R.
805 M. W., Guggenberger, G., and McDowell, W. H.: Sources and the flux pattern of dissolved carbon in
806 rivers of the Yenisey basin draining the Central Siberian Plateau, *Environmental Research Letters*, 6,
807 45212–45226, <https://doi.org/10.1088/1748-9326/6/4/045212>, 2011.
- 808 Pulliainen, J., Luojus, K., Derksen, C., Mudryk, L., Lemmetyinen, J., Salminen, M., Ikonen, J., Takala,
809 M., Cohen, J., Smolander, T., and Norberg, J.: Patterns and trends of Northern Hemisphere snow

810 mass from 1980 to 2018, *Nature* 2020 581:7808, 581, 294–298, [https://doi.org/10.1038/s41586-](https://doi.org/10.1038/s41586-020-2258-0)
811 020-2258-0, 2020.

812 Rantanen, M., Karpechko, A. Y., Lipponen, A., Nordling, K., Hyvärinen, O., Ruosteenoja, K., Vihma, T.,
813 and Laaksonen, A.: The Arctic has warmed nearly four times faster than the globe since 1979,
814 *Commun Earth Environ*, 3, 1–10, <https://doi.org/10.1038/s43247-022-00498-3>, 2022.

815 Räsänen, A., Manninen, T., Korkiakoski, M., Lohila, A., and Virtanen, T.: Predicting catchment-scale
816 methane fluxes with multi-source remote sensing, *Landscape Ecology*, 36, 1177–1195,
817 <https://doi.org/10.1007/S10980-021-01194-X/FIGURES/4>, 2021.

818 Rosset, T., Gandois, L., Le Roux, G., Teisserenc, R., Durantez Jimenez, P., Camboulive, T., and Binet,
819 S.: Peatland Contribution to Stream Organic Carbon Exports From a Montane Watershed, *Journal of*
820 *Geophysical Research: Biogeosciences*, 124, 3448–3464, <https://doi.org/10.1029/2019JG005142>,
821 2019.

822 Ruckhaus, M., Seybold, E. C., Underwood, K. L., Stewart, B., Kincaid, D. W., Shanley, J. B., Li, L., and
823 Perdrial, J. N.: Disentangling the responses of dissolved organic carbon and nitrogen concentrations
824 to overlapping drivers in a northeastern United States forested watershed, *Frontiers in Water*, 5,
825 2023.

826 Sallinen, A., Akanegbu, J., Marttila, H., and Tahvanainen, T.: Recent and future hydrological trends of
827 aapa mires across the boreal climate gradient, *Journal of Hydrology*, 617, 129022,
828 <https://doi.org/10.1016/j.jhydrol.2022.129022>, 2023.

829 Shatilla, N. J. and Carey, S. K.: Assessing inter-annual and seasonal patterns of DOC and DOM quality
830 across a complex alpine watershed underlain by discontinuous permafrost in Yukon, Canada,
831 *Hydrology and Earth System Sciences*, 23, 3571–3591, <https://doi.org/10.5194/hess-23-3571-2019>,
832 2019.

833 Shatilla, N. J., Tang, W., and Carey, S. K.: Multi-year high-frequency sampling provides new runoff
834 and biogeochemical insights in a discontinuous permafrost watershed, *Hydrological Processes*, 37,
835 e14898, <https://doi.org/10.1002/hyp.14898>, 2023.

836 Shogren, A. J., Zarnetske, J. P., Abbott, B. W., Iannucci, F., and Bowden, W. B.: We cannot shrug off
837 the shoulder seasons: Addressing knowledge and data gaps in an Arctic headwater, *Environmental*
838 *Research Letters*, 15, 104027, <https://doi.org/10.1088/1748-9326/ab9d3c>, 2020.

839 Shogren, A. J., Zarnetske, J. P., Abbott, B. W., Iannucci, F., Medvedeff, A., Cairns, S., Duda, M. J., and
840 Bowden, W. B.: Arctic concentration–discharge relationships for dissolved organic carbon and nitrate
841 vary with landscape and season, *Limnology and Oceanography*, 66, S197–S215,
842 <https://doi.org/10.1002/lno.11682>, 2021.

843 Speetjens, N. J., Tanski, G., Martin, V., Wagner, J., Richter, A., Hugelius, G., Boucher, C., Lodi, R.,
844 Knoblauch, C., Koch, B. P., Wünsch, U., Lantuit, H., and Vonk, J. E.: Dissolved organic matter
845 characterization in soils and streams in a small coastal low-Arctic catchment, *Biogeosciences*, 19,
846 3073–3097, <https://doi.org/10.5194/bg-19-3073-2022>, 2022.

847 Tan, A., Adam, J. C., and Lettenmaier, D. P.: Change in spring snowmelt timing in Eurasian Arctic
848 rivers, *Journal of Geophysical Research: Atmospheres*, 116, D03101,
849 <https://doi.org/10.1029/2010JD014337>, 2011.

850 Tank, S. E., Striegl, R. G., McClelland, J. W., and Kokelj, S. V.: Multi-decadal increases in dissolved
851 organic carbon and alkalinity flux from the Mackenzie drainage basin to the Arctic Ocean,
852 *Environmental Research Letters*, 11, 054015, <https://doi.org/10.1088/1748-9326/11/5/054015>,
853 2016.

854 Tiefenbacher, A., Weigelhofer, G., Klik, A., Mabit, L., Santner, J., Wenzel, W., and Strauss, P.:
855 Antecedent soil moisture and rain intensity control pathways and quality of organic carbon exports
856 from arable land, *CATENA*, 202, 105297, <https://doi.org/10.1016/j.catena.2021.105297>, 2021.

857 Vaughan, M. C. H., Bowden, W. B., Shanley, J. B., Vermilyea, A., Sleeper, R., Gold, A. J., Pradhanang,
858 S. M., Inamdar, S. P., Levia, D. F., Andres, A. S., Birgand, F., and Schroth, A. W.: High-frequency
859 dissolved organic carbon and nitrate measurements reveal differences in storm hysteresis and
860 loading in relation to land cover and seasonality, *Water Resources Research*, 53, 5345–5363,
861 <https://doi.org/10.1002/2017WR020491>, 2017.

862 Vihma, T., Screen, J., Tjernström, M., Newton, B., Zhang, X., Popova, V., Deser, C., Holland, M., and
863 Prowse, T.: The atmospheric role in the Arctic water cycle: A review on processes, past and future
864 changes, and their impacts, *Journal of Geophysical Research: Biogeosciences*, 121, 586–620,
865 <https://doi.org/10.1002/2015JG003132>, 2016.

866 Ward, A. S., Wondzell, S. M., Schmadel, N. M., and Herzog, S. P.: Climate Change Causes River
867 Network Contraction and Disconnection in the H.J. Andrews Experimental Forest, Oregon, USA,
868 *Frontiers in Water*, 2, 2020.

869 Williams, G. P.: Sediment concentration versus water discharge during single hydrologic events in
870 rivers, *Journal of Hydrology*, 111, 89–106, [https://doi.org/10.1016/0022-1694\(89\)90254-0](https://doi.org/10.1016/0022-1694(89)90254-0), 1989.

871 de Wit, H. A., Valinia, S., Weyhenmeyer, G. A., Futter, M. N., Kortelainen, P., Austnes, K., Hessen, D.
872 O., Räike, A., Laudon, H., and Vuorenmaa, J.: Current Browning of Surface Waters Will Be Further
873 Promoted by Wetter Climate, *Environ. Sci. Technol. Lett.*, 3, 430–435,
874 <https://doi.org/10.1021/acs.estlett.6b00396>, 2016.

875 Zarnetske, J. P., Bouda, M., Abbott, B. W., Saiers, J., and Raymond, P. A.: Generality of Hydrologic
876 Transport Limitation of Watershed Organic Carbon Flux Across Ecoregions of the United States,
877 *Geophysical Research Letters*, 45, 11,702–11,711, <https://doi.org/10.1029/2018GL080005>, 2018.

878